1

THE MEMBRANE EQUATION

Any physical or biophysical mechanism instantiating an information processing system that needs to survive in the real world must obey several constraints: (1) it must operate at high speeds, (2) it must have a rich repertoire of computational primitives, with the ability to implement a variety of linear and nonlinear, high-gain, operations, and (3) it must interface with the physical world—in the sense of being able to represent sensory input patterns accurately and translate the result of the computations into action, that is motor output (Keyes, 1985).

The membrane potential is the one physical variable within the nervous system that fulfills these three requirements: it can vary rapidly over large distances (e.g., an action potential changes the potential by 100 mV within 1 msec, propagating up to 1 cm or more down an axon within that time), and the membrane potential controls a vast number of nonlinear gates—ionic channels—that provide a very rich substrate for implementing nonlinear operations. These channels transduce visual, tactile, auditory, and olfactory stimuli into changes of the membrane potential, and such voltage changes back into the release of neurotransmitters or the contraction of muscles.

This is not to deny that ionic fluxes, or chemical interactions of various substances with each other, are not crucial to the working of the brain. They are, and we will study some of these mechanisms in Chap. 11. Yet the membrane potential is the incisive variable that serves as primary vehicle for the neuronal operations underlying rapid computations—at the fraction of a second time scale—in the brain.

We will introduce the reader in a very gentle manner to the electrical properties of nerve cells by starting off with the very simplest of all neuronal models, consisting of nothing more than a resistance and a capacitance (a so-called *RC circuit*). Yet endowed with synaptic input, this model can already implement a critical nonlinear operation, *divisive normalization* and *gain control.*

1.1 Structure of the Passive Neuronal Membrane

As a starting point, we choose a so-called *point* representation of a neuron. Here, the spatial dependency of the neuron is reduced to a single point or compartment. Such an

approximation would be valid, for instance, if we were investigating a small, spherical cell without a significant dendritic tree.

1.1.1 Resting Potential

The first thing we notice once we managed to penetrate into this cell with a wire from which we can record (termed an intracellular *microelectrode*) is the existence of an electrical potential across this membrane. Such experiments, carried out in the late 1930s by Cole and Curtis (1936) in Woods Hole, Massachusetts, and by Hodgkin and Huxley (1939) on the other side of the Atlantic, demonstrated that almost always, the membrane potential, defined as the difference between the intracellular and the extracellular potentials, or

$$V_m(t) = V_i(t) - V_e(t), \tag{1.1}$$

is negative. Here t stands for time. In particular, at rest, all cells, whether neurons, glia or muscle cells, have a negative resting potential, symbolized throughout the book as V_{rest}. Depending on the circumstances, it can be as high as -30 mV or as low as -90 mV. Note that when we say the cell is at "rest," it is actually in a state of dynamic equilibrium. Ionic currents are flowing across the membrane, but they balance each other, in such a manner that the net current flowing across the membrane is zero. Maintaining this equilibrium is a major power expenditure for the nervous system. Half of the metabolic energy consumed by a mammalian brain has been estimated to be due to the membrane-bound pumps that are responsible for the upkeep of the underlying ionic gradients (Ames, 1997).

The origin of V_{rest} lies in the differential distribution of ions across the membrane, which we do not further describe here (see Sec. 4.4 and Hille, 1992). V_{rest} need not necessarily be fixed. Indeed, we will discuss in Sec. 18.3 conditions under which a network of cortical cells can dynamically adjust their resting potentials.

1.1.2 Membrane Capacity

What is the nature of the membrane separating the intracellular cytoplasm from the extracellular milieu (Fig. 1.1)? The two basic constitutive elements of biological membranes, whether from the nervous system or from nonneuronal tissues such as muscle or red blood cells, whether prokaryotic or eukaryotic, are *proteins* and *lipids* (Gennis, 1989).

The backbone of the membrane is made of two layers of phospholipid molecules, with their polar heads facing the intracellular cytoplasm and the extracellular space, thereby separating the internal and external conducting solutions by a 30–50-Å-thin insulating layer. We know that whenever a thin insulator is keeping charges apart, it will act like a *capacitance*. The capacitance C is a measure of how much charge Q needs to be distributed across the membrane in order for a certain potential V_m to build up. Or, conversely, the membrane potential V_m allows the capacitance to build up a charge Q on both sides of the membrane, with

$$Q = CV_m. \tag{1.2}$$

In membrane biophysics, the capacitance is usually specified in terms of the *specific membrane capacitance* C_m, in units of microfarads per square centimeter of membrane area (μF/cm^2). The actual value of C can be obtained by multiplying C_m by the total membrane area. The thickness and the dielectric constant of the bilipid layer determine the numerical value of C_m. For the simplest type of capacitance formed by two parallel plates, C_m scales

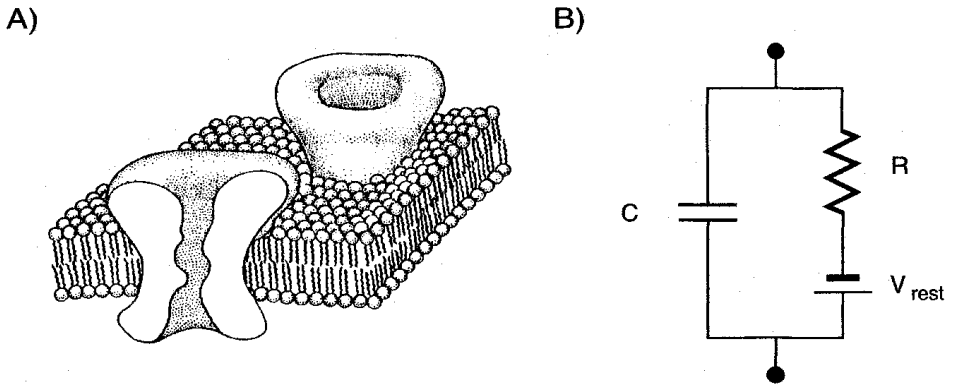

Fig. 1.1 Nature of the Passive Neuronal Membrane **(A)** Schematic representation of a small patch of membrane of the types enclosing all cells. The 30–50 Å thin bilayer of lipids isolates the extracellular side from the intracellular one. From an electrical point of view, the resultant separation of charge across the membrane acts akin to a capacitance. Proteins inserted into the membrane, here ionic channels, provide a conduit through the membrane. Reprinted by permission from Hille (1992). **(B)** Associated lumped electrical circuit for this patch, consisting of a capacitance and a resistance in series with a battery. The resistance mimics the behavior of voltage-independent ionic channels inserted throughout the membrane and the battery accounts for the cell's resting potential V_{rest}.

inversely with the thickness separating the charges (the thinner the distance between the two plates, the stronger the mutual attraction of the charges across the insulating material). As discussed in Appendix A, the specific capacitance per unit area of biological membranes is between 0.7 and 1 μF/cm^2. For the sake of convenience, we adopt the latter, simple to remember, value. This implies that a spherical cell of 5-μm radius with a resting potential of -70 mV stores about -0.22×10^{-12} coulomb of charge just below the membrane and an equal but opposite amount of charge outside.

When the voltage across the capacitance changes, a current will flow. This *capacitive current*, which moves on or off the capacitance, is obtained by differentiating Eq. 1.2 with respect to time (remember that current is the amount of charge flowing per time),

$$I_C = C\frac{dV_m(t)}{dt}. \tag{1.3}$$

For a fixed current, the existence of the membrane capacitance imposes a constraint on how rapidly V_m can change in response to this current; the larger the capacitance, the slower the resultant voltage change.

It is important to realize that there is never any actual movement of charge across the insulating membrane. When the voltage changes with time, the charge changes and a current will flow, in accordance with Eq. 1.3, but never directly across the capacitance. The charge merely redistributes itself across the two sides by way of the rest of the circuit.

Can any current flow directly across the bilipid layers? As detailed in Appendix A, the extremely high resistivity of the lipids prevents passages of any significant amount of charge across the membrane. Indeed, the specific resistivity of the membrane is approximately one billion times higher than that of the intracellular cytoplasm. Thus, from an electrical point of view, the properties of the membrane can be satisfactorily described by a sole element: a capacitance.

1.1.3 Membrane Resistance

With no other components around, life would indeed be dull. What endows a large collection of squishy cells with the ability to move and to think are the all-important *proteins* embedded within the membrane. Indeed, they frequently penetrate the membrane, allowing ions to pass from one side to the other (Fig. 1.1). Protein molecules, making up anywhere from 20 to 80% (dry weight) of the membrane, subserve an enormous range of specific cellular functions, including ionic channels, enzymes, pumps, and receptors. They act as doors or gates in the lipid barrier through which particular information or substances can be transferred from one side to the other. As we shall see later on, a great variety of such "gates" exists, with different keys to open them. For now, we are interested in those membrane proteins that act as ionic *channels* or *pores*, enabling ions to travel from one side of the membrane to the other. We will discuss the molecular nature of these channels in more detail in Chap. 8.

For now, we will summarily describe the current flow through these channels by a simple linear resistance R. Since we also have to account for the resting potential of the cell, the simplest electrical description of a small piece of membrane includes three elements, C, R, and V_{rest} (Fig. 1.1). Such a circuit describes a *passive* membrane in contrast to *quasi-active* and *active* membranes, which contain, respectively, linear, inductance-like, and nonlinear voltage-dependent membrane components. For obvious reasons, it is also sometimes known as an *RC circuit*. Fortuitously, the membranes of quite a few cells can be mimicked by such *RC* circuits, at least under some limited conditions.

The membrane resistance is usually specified in terms of the *specific membrane resistance* R_m, expressed in terms of resistance times unit area (in units of $\Omega \cdot \text{cm}^2$). R is obtained by dividing R_m by the area of the membrane being considered. The inverse of R_m is known as the passive conductance per unit area of dendritic membrane or, for short, as the *specific leak conductance* $G_m = 1/R_m$ and is measured in units of siemens per square centimeter (S/cm^2).

1.2 A Simple *RC* Circuit

Let us now carry out a virtual electrophysiological experiment. Assume that we have identified a small spherical neuron of diameter d and have managed to insert a small electrode into the cell without breaking it up. Under the conditions of our experiments, we have reasons to believe that its membrane acts passively. We would like to know what happens if we inject current $I_{\text{inj}}(t)$ through the microelectrode directly into the cell. This electrode can be thought of as an ideal *current source* (in contrast to an ideal voltage source, such as a battery).

How can we describe the dynamics of the membrane potential $V_m(t)$ in response to this current? The cell membrane can be conceptualized as being made up from many small *RC* circuits (Fig. 1.2A). Because the dimensions of the cell are so small, the electrical potential across the membrane is everywhere the same and we can neglect any spatial dependencies; physiologists will say the cell is *isopotential*. This implies that the electrical behavior of the cell can be adequately described by a single *RC* compartment with a current source (Fig. 1.2B). The net resistance R is determined by the specific membrane resistance R_m divided by the total membrane area πd^2 (since the current can flow out through any one part of the membrane) while the total capacitance C is given by C_m times the membrane area.

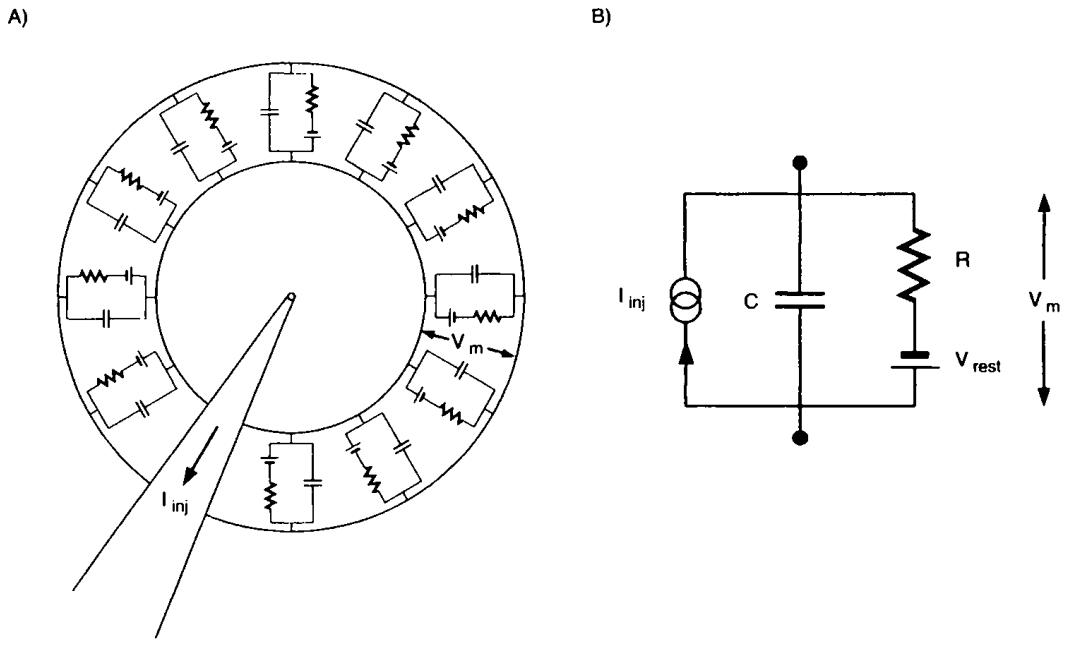

Fig. 1.2 Electrical Structure of a Small Passive Neuron **(A)** Equivalent electrical model of a spherical cell with passive membrane. An intracellular electrode delivers current to the cell. By convention, an outward current is positive; thus, the arrow. We assume that the dimensions of the cell are small enough so that spatial variations in the membrane potential can be neglected. **(B)** Under these conditions, the cell can be reduced to a single *RC* compartment in series with an ideal current source I_{inj}.

It is straightforward to describe the dynamics of this circuit by applying *Kirchhoff's current law*, which states that the sum of all currents flowing into or out of any electrical node must be zero (the current cannot disappear, it has to go somewhere). The current across the capacitance is given by expression 1.3. The current through the resistance is given by *Ohm's law*,

$$I_R = \frac{V_m - V_{rest}}{R} . \tag{1.4}$$

Note that the potential across the resistance is not equal to V_m, but to the difference between the membrane potential and the fictive battery V_{rest}, which accounts for the resting potential. Due to conservation of current, the capacitive and resistive currents must be equal to the external one, or

$$C\frac{dV_m(t)}{dt} + \frac{V_m(t) - V_{rest}}{R} = I_{inj}(t) . \tag{1.5}$$

With $\tau = RC$, with units of $\Omega \cdot F = sec$, we can rewrite this as

$$\tau\frac{dV_m(t)}{dt} = -V_m(t) + V_{rest} + RI_{inj}(t) . \tag{1.6}$$

A minor, but important detail is the sign of the external current (after all, we could have replaced $+I_{inj}$ by $-I_{inj}$ in Eq. 1.6). By convention, an outward current, that is positive charge flowing from inside the neuron to the outside, is represented as a positive current. An outward going current that is delivered through an intracellular electrode will make the inside of the cell more positive; the physiologist says that the cell is *depolarized*. Conversely,

an inward directed current supplied by the same electrode, plotted by convention in the negative direction, will make the inside more negative, that is, it will *hyperpolarize* the cell. If the current is not applied from an external source but is generated by a membrane conductance, the situation is different (see Chap. 5).

Due to the existence of the battery V_{rest}, the electrical diagram in Fig. 1.2B does *not*, formally speaking, constitute a *passive* circuit, since its current-voltage (I–V) relationship is not restricted to the first and third quadrants of the I–V plane. This implies that power is needed to maintain this I–V relationship, ultimately supplied by the differential distributions of ions across the membrane. Because the I–V relationship has a nonzero, positive derivative for every value of V_m, it is known as an *incrementally passive* device. This point is not without interest, since it relates to the stability of circuits built using such components (Wyatt, 1992). We here do not take a purist point of view, and we will continue to refer to a membrane whose equivalent circuit diagram is similar to that of Figs. 1.1B and 1.2B as passive.

Equation 1.6 is known as the *membrane equation* and constitutes a first-order, ordinary differential equation. With the proper initial conditions, it specifies an unique voltage trajectory. Let us assume that the membrane potential starts off at $V_m(t = 0) = V_{\text{rest}}$. We can replace this into Eq. 1.6 and see that in the absence of any input ($I_{\text{inj}} = 0$) this assumption yields $dV_m/dt = 0$, that is, once at V_{rest}, the system will remain at V_{rest} in the absence of any input. This makes perfect sense. So now let us switch on, at $t = 0$, a step of current of constant amplitude I_0. We should remember from the theory of ordinary differential equations that the most general form of the solution of Eq. 1.6 can be expressed as

$$V_m(t) = v_0 e^{-t/\tau} + v_1 \tag{1.7}$$

where v_0 and v_1 depend on the initial conditions. Replacing this into Eq. 1.6 and canceling identical variables on both sides leaves us with

$$v_1 = V_{\text{rest}} + RI_0 . \tag{1.8}$$

We obtain the value of v_0 by imposing the initial condition $V_m(t = 0) = v_0 + v_1 = V_{\text{rest}}$. Defining the steady-state potential in response to the current as $V_\infty = RI_0$, we have solved for the dynamics of V_m for this cell,

$$V_m(t) = V_\infty(1 - e^{-t/\tau}) + V_{\text{rest}} . \tag{1.9}$$

This equation tells us that the time course of the deviation of the membrane potential from its resting state, that is, $V_m(t) - V_{\text{rest}}$, is an exponential function in time, with a time constant equal to τ. Even though the current changed instantaneously from zero to I_0, the membrane potential cannot follow but plays catch up. This is demonstrated graphically in Fig. 1.3. How slowly V_m changes is determined by the product of the membrane resistance and the capacitance; the larger the capacitance, the larger the current that goes toward charging up C. Note that τ is independent of the size of the cell,

$$\tau = RC = R_m C_m . \tag{1.10}$$

As we will discuss in considerable detail in later chapters, passive time constants range from 1 to 2 msec in neurons that are specialized in processing high-fidelity temporal information to 100 msec or longer for cortical neurons recorded under slice conditions. A

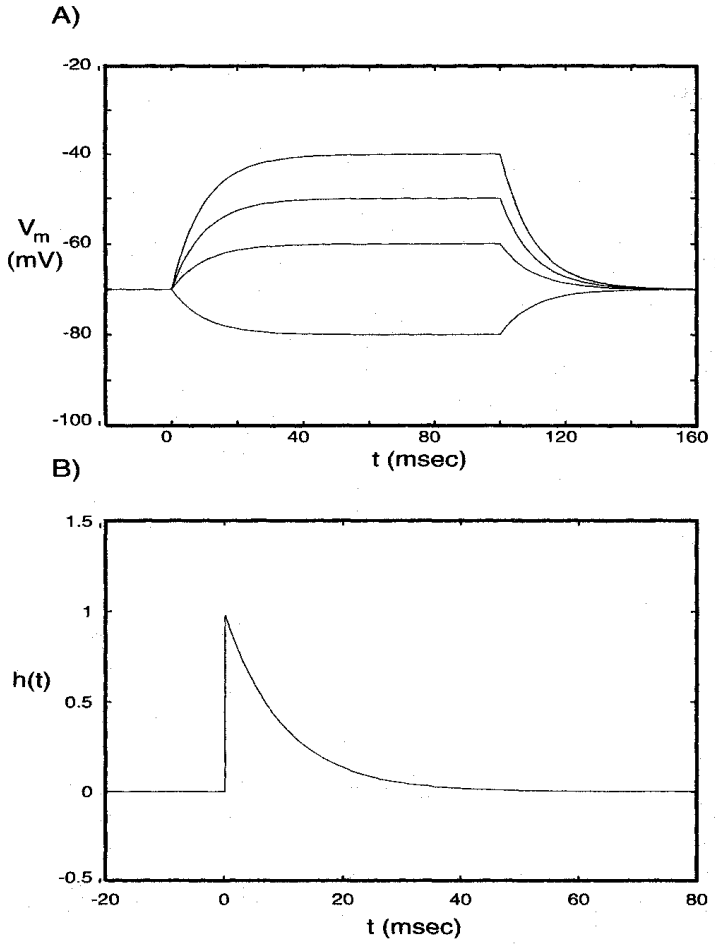

Fig. 1.3 Behavior of an *RC* Circuit **(A)** Evolution of the membrane potential $V_m(t)$ in the single *RC* compartment of Fig. 1.2B when a current step of different amplitudes I_0 (see Eq. 1.9) is switched on at $t = 0$ and turned off at 100 msec. Initially, the membrane potential is at $V_{\text{rest}} = -70$ mV. We here assume $R = 100$ MΩ, $C = 100$ pF, $\tau = 10$ msec, and four different current amplitudes, $I_0 = -0.1, 0.1, 0.2$, and 0.3 nA. **(B)** Normalized *impulse response* or *Green's function* (Eq. 1.17) associated with the *RC* circuit of Fig. 1.2B. The voltage $V_m(t)$ in response to any current input $I_{\text{inj}}(t)$ can be obtained by convolving this function with the input.

typical range for τ recorded from cortical pyramidal cells in the living animal[1] is between 10 and 20 msec.

Remember the origin of the membrane capacitance in the molecular dimensions of the bilipid membrane. A thicker membrane would lead to a smaller value for C_m and faster temporal responses.[2]

The final voltage level in response to the current step is $RI_0 + V_{\text{rest}}$ (from Ohm's law). If $I_0 > 0$, the cell will depolarize (that is, $V_\infty > V_{\text{rest}}$), whereas for $I_0 < 0$, the converse occurs. The resistance R is also termed the *input resistance* of the cell; the larger R, the larger the voltage change in response to a fixed current. The input resistance at the cell bodies of neurons, obtained by dividing the steady-state voltage change by the current causing it, ranges from a few megaohms for the very large motoneurons in the spinal cord to hundreds of megaohms for cortical spiny stellate cells or cerebellar granule cells.

1. This is called *in vivo*. Such experiments need to be distinguished from the cases in which a very thin slice is taken from an animal's brain, placed in a dish, and perfused with a nutrient solution. This would be termed an *in vitro* experiment.

2. As an aside to the neuromorphic engineers among us designing analog integrated electronic circuits, $C_m = 1\ \mu\text{F/cm}^2$ is about 20 times higher than the specific capacitance obtained by sandwiching a thin layer of silicon dioxide between two layers of poly silicon using a standard 2.0 or 1.2 μm CMOS process (Mead, 1989).

What happens if, after the membrane potential reaches its steady-state value V_∞, the current is switched off at time t_{off}? An analysis similar to the above shows that the membrane potential returns to V_{rest} with an exponential time course; that is,

$$V_m(t) = V_\infty e^{-(t-t_{off})/\tau} + V_{rest} \tag{1.11}$$

for $t \geq t_{off}$. (This can be confirmed by placing this solution into Eq. 1.6; see also Fig. 1.3A.)

Now that we know the evolution of the membrane potential for a current step, we would like to know the solution in the general case of some time-dependent current input $I_{inj}(t)$. Are we condemned to solve Eq. 1.6 explicitly for every new function $I_{inj}(t)$ that we use? Fortunately not; because the *RC* circuit we have been treating here is a shift-invariant, linear system, we can do much better.

1.3 *RC* Circuits as Linear Systems

Linearity is an important property of certain systems that allows us—in combination with shift invariance—to completely characterize their behavior to *any* input in terms of the system's *impulse response* or *Green's function* (named after a British mathematician living at the beginning of the nineteenth century). Since the issue of linear and nonlinear systems runs like a thread through this monograph, we urge the reader who has forgotten these concepts to quickly skim through Appendix B, which summarizes the most relevant points.

1.3.1 Filtering by RC Circuits

Let us compute the voltage response of the *RC* circuit of Fig. 1.2B in response to a current impulse $\delta(t)$. We will simplify matters by only considering the deviation of the membrane potential from its resting state V_{rest}. Here and throughout the book we use $V(t) = V_m(t) - V_{rest}$ when we are dealing with the potential relative to rest and reserve $V_m(t)$ for the absolute potential. This transforms Eq. 1.6 into

$$\tau \frac{dV(t)}{dt} = -V(t) + R\delta(t)\,. \tag{1.12}$$

We can transform this equation into Fourier space, where $\tilde{V}(f)$ corresponds to the Fourier transform of the membrane potential (for a definition, see Appendix B). Remembering that the $dV(t)/dt$ term metamorphoses into $i2\pi\,\tilde{V}(f)\hat{V}(P)$, where $i^2 = -1$, we have

$$\tilde{V}(f) = \frac{R}{1 + i2\pi f\tau}\,. \tag{1.13}$$

A simple way to conceptualize this is to think of the input as a sinusoidal current of frequency f; $I_{inj}(t) = \sin(2\pi f t)$. Since the system is linear, it responds by a sinusoidal change of potential at the same frequency f, but of different amplitude and shifted in time: $V(t) = \tilde{A}(f)\sin(2\pi f t + \tilde{\phi}(f))$. The amplitude of the voltage response at this frequency, termed $\tilde{A}(f)$, is given by

$$|\tilde{A}(f)| = \frac{R}{\sqrt{1 + (2\pi f\tau)^2}} \tag{1.14}$$

and its phase by

$$\tilde{\phi}(f) = -\arctan(2\pi f\tau)\,. \tag{1.15}$$

In the general case of an arbitrary input current, one can define the complex function $\tilde{A}(f)$ as the ratio of the Fourier transform of the voltage transform to the Fourier transform of the injected current,

$$\tilde{A}(f) = \frac{\tilde{V}(f)}{\tilde{I}_{\text{inj}}(f)}\,. \tag{1.16}$$

$\tilde{A}(f)$ is usually referred to as the *input impedance* of the system. Its value for a sustained or dc current input, $\tilde{A}(f = 0) = R$, is known as the *input resistance* and is a real number. It is standard engineering practice to refer to the inverse of the input impedance as the *input admittance* and to the inverse of the input resistance as the *input conductance* in units of siemens (S).

Does this definition of $\tilde{A}$ make sense? Let us look at two extreme cases. If we subject the system to a sustained current injection, the change in voltage in response to a sustained input current I is proportional to R, Ohm's law. Conversely, what happens if we use a sinusoidal that has a very high frequency f? The amplitude of the voltage change becomes less and less since at high frequencies the capacitance essentially acts like a short circuit. In the limit of $f \to \infty$, the impedance goes to zero.

For intermediate values of f, the amplitude smoothly interpolates between R and 0. In other words, our circuit acts like a *low-pass* filter, preferentially responding to slower changing inputs and severely attenuating faster ones: $|\tilde{A}(f)|$ is a strictly monotonically decreasing function of the frequency f.

Experimentally, the impedance can be obtained by injecting a sinusoidal current of frequency f and measuring the induced voltage at the same frequency. The ratio of the voltage to the current corresponds to $|\tilde{A}(f)|$. The use of impedances to describe the electrical behavior of neurons and, in particular, of muscle cells has a long tradition going back to the 1930s (Cole and Curtis, 1936; Falk and Fatt, 1964; Cole, 1972).

The result of such a procedure, carried out in a regular firing cell in a slice taken from the visual cortex of the guinea pig, is shown in Fig. 1.4. Carandini and his colleagues (1996) injected either sinusoidal currents or a noise stimulus into these cells and recorded the resultant somatic membrane potential (in the presence of spikes). Given their very fast time scale, somatic action potentials do not contribute appreciably to the total power of the voltage signal. Indeed, when stimulating with a sine wave at frequency f, the power of the voltage response at all higher frequencies was only 3.8% (median) of the power of the fundamental f. This implies that when judged by the membrane potential and not by the firing rate, and only considering input and output at the soma, at least some cortical cells can be quite well approximated by a linear filter (Carandini et al., 1996).

This is surprising, given the presence of numerous voltage-dependent conductances at the soma and in the dendritic tree. It is, however, not uncommon in neurobiology to find that despite of—or, possibly because of—a host of concatenated nonlinearities, the overall system behaves quite linearly (see Sec. 21.1.3). Sometimes one has the distinct impression that evolution wanted to come up with some overall linear mechanism, despite all the existing nonlinearities.

We will study later how adding a simple, absolute voltage threshold to the *RC* compartment that gives rise to an output spike accounts surprisingly well for the spiking behavior

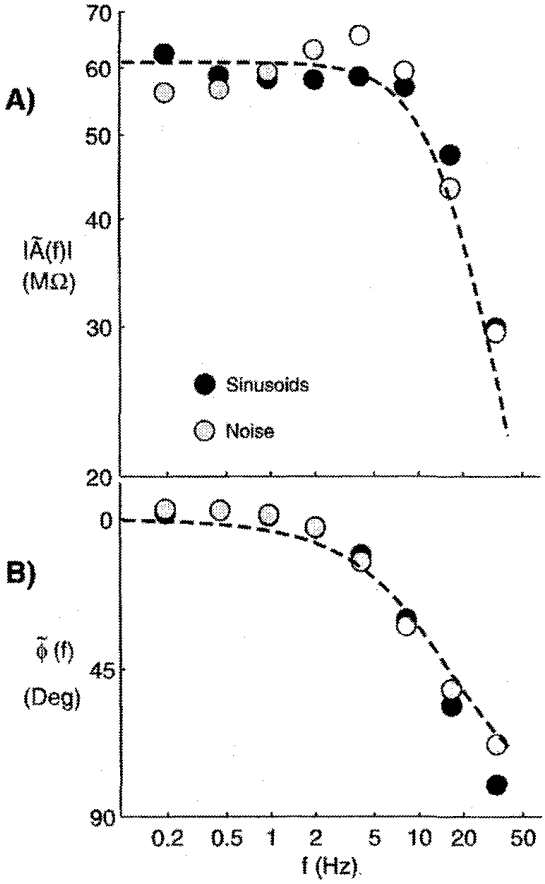

Fig. 1.4 CORTICAL CELLS BEHAVE LIKE AN *RC* CIRCUIT When either noise or sinusoidal currents are injected into the cell body of regularly firing cells in guinea pig visual cortex, the membrane potential can be adequately modeled as resulting from convolving the current input by a low-pass filter of the sort described in Eqs. 1.14 and 1.15 (dashed lines; here with $R = 58.3$ MΩ and $\tau = 9.3$ msec; $V_{\text{rest}} = -70.7$ mV; Carandini et al., 1996). **(A)** The amplitude of the filter and **(B)** its phase. The noise current curve reveals a shallow peak at around 8 Hz. We conclude that from the point of view of somatic input-output, these cells can be reasonably well described by a single *RC* compartment. The responses were obtained by computing the first harmonic of the membrane potential response and dividing by the current. The power of the first harmonic was between 9 and 141 times the power of the higher harmonics. Reprinted by permission from Carandini et al., (1996).

of such cells. This simplest model of a spiking neuron, known as a *leaky integrate-and-fire* unit, is so important that it deserves its own detailed treatment in Chap. 14.

We can recover the Green's function $h(t)$ of the *RC* compartment by applying the inverse Fourier transform to Eq. 1.13, which results in

$$h(t) = \frac{1}{C} e^{-t/\tau} \tag{1.17}$$

for $t \geq 0$ and 0 for negative times (the units of the Green's function are ohms per second (Ω/sec)). Conceptually, the extent of this filter, that is, the temporal duration over which this filter is significantly different from zero, indicates to what extent the distant past influences the present behavior of the system. For a decaying exponential as in an *RC* circuit, an event that happened three time constants ago (at $t = -3\tau$) will have roughly 1/20 the effect of something that just occurred (Fig. 1.3B). This is expected in a circuit that implements a low-pass operation. Input is integrated in time, with long ago events having exponentially less impact than more recent ones.

1.4 Synaptic Input

So far, we have not considered how the output of one neuron provides input to the next one. Fast communication among two neurons occurs at specialized contact zones, termed *synapses*. Synapses are the elementary structural and functional units for the construction of

neuronal circuits. Conventional point-to-point synaptic interactions come in two different flavors: *electrical synapses*—also referred to as *gap junctions*—and the much more common *chemical synapses*. At about 1 billion chemical synapses per cubic millimeter of cortical grey matter, there are lots of synapses in the nervous system (on the order of 10^{15} for a human brain). In order to give the reader an appreciation of this, Fig. 1.5 is a photomicrograph of a small patch of the monkey retina at the electron-microscopic level, with a large number of synapses visible. Synapses are very complex pieces of machinery that can keep track of their history of usage over considerable time scales. In this chapter, we introduce fast, voltage independent chemical synapses from the point of view of the postsynaptic cell, deferring a more detailed account of synaptic biophysics, as well as voltage dependent synapses and electrical synapses, to Chap. 4, and an account of their adapting and plastic properties to Chap. 13.

Upon activation of a fast, chemical synapse, one can observe a rapid and transient change in the *postsynaptic* potential. Here, postsynaptic simply means that we are observing this signal on the "far" or "output" side of the synapse; the "input" part of a synapse is referred to as the *presynaptic* terminal. When the synapse is an excitatory one, the membrane potential rapidly depolarizes, returning more slowly to its resting state: an *excitatory postsynaptic potential* (EPSP) has occurred. Conversely, at an inhibitory synapse, the membrane will typically be transiently hyperpolarized, resulting in an *inhibitory postsynaptic potential* (IPSP). These EPSPs and IPSPs are caused by so-called *excitatory* and *inhibitory postsynaptic currents* (EPSCs and IPSCs), triggered by the spiking activity in the presynaptic cell.

Figure 1.6 illustrates some of the properties of a population of depolarizing synapses between the axons of granule cells, also called *mossy fibers*, and a CA3 hippocampal

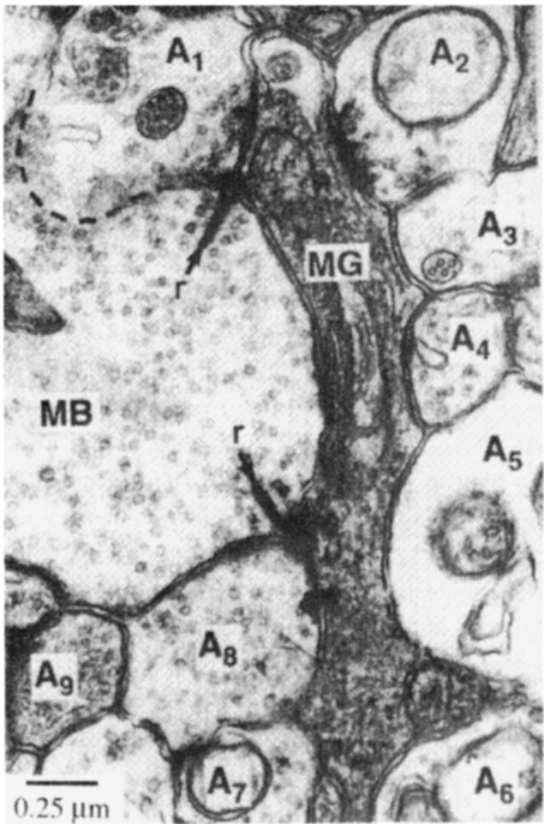

Fig. 1.5 Synapses among Retinal Neurons Electron microscopic photograph of a few square micrometers of tissue in the central portion of the retina in the monkey. Here a midget bipolar cell (**MB**) makes two *ribbon synapses* onto a midget ganglion cell (**MG**). It is surrounded by nine processes belonging to amacrine cells ($\mathbf{A}_1$ to $\mathbf{A}_9$). Some of these feed back onto the bipolar cell (e.g., $\mathbf{A}_8$), some feed forward onto the ganglion cell (e.g., $\mathbf{A}_1$), some do both, and some also contact each other (e.g., $\mathbf{A}_2 \rightarrow \mathbf{A}_3$). Since neither the bipolar cell nor the amacrine cell processes have been shown to generate action potentials, these synapses are all of the analog variety, in distinction to synapses in the more central part of the nervous system that typically transform an action potential into a graded, postsynaptic signal. Reprinted by permission from Calkins and Sterling (1996).

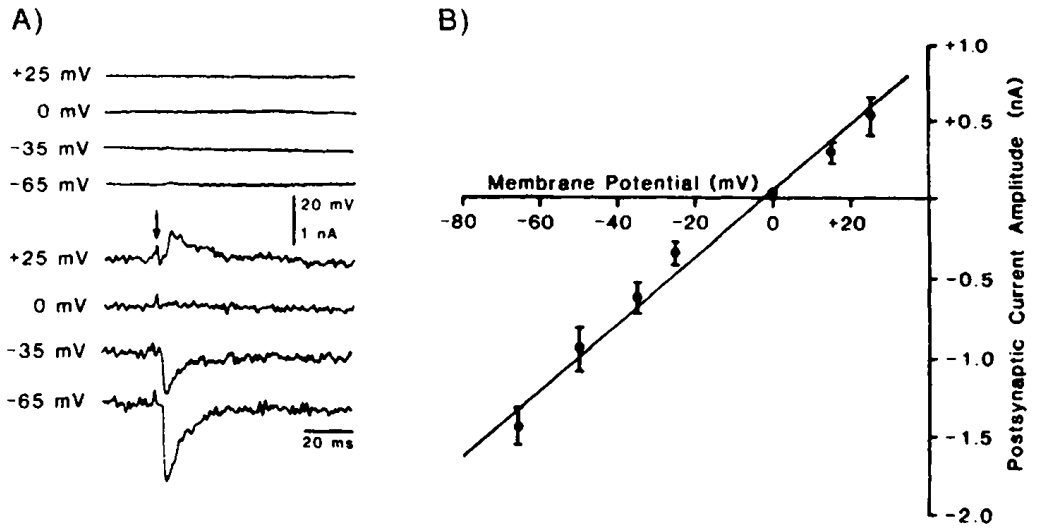

Fig. 1.6 A Fast Excitatory Synaptic Input Excitatory postsynaptic current (EPSC) caused by the simultaneous activation of synapses (arrow) made by the mossy fibers onto CA3 pyramidal cells in the rodent hippocampus (Brown and Johnston, 1983). This classical experiment showed how a central synapse can be successfully voltage clamped. **(A)** The voltage-clamp setup stabilizes—via electronic feedback control—the membrane potential at a fixed value. Here four experiments are shown, carried out at the holding potentials indicated at the left. The current that is drawn to keep the membrane potential constant, termed the clamp current, corresponds to the negative EPSC. It is maximal at negative potentials and reverses sign around zero. The synaptic current rises within 1 msec to its peak value, decaying to baseline over 20–30 msec. The experiments were carried out in the presence of pharmacological agents that blocked synaptic inhibition. **(B)** When the peak EPSC is plotted against the holding potential, an approximately linear relationship emerges; the regression line yields an x-axis intercept of -1.9 mV and a slope of 20.6 nS. Thus, once the synaptic reversal potential is accounted for, Ohm's law appears to be reasonably well obeyed. We conclude that synaptic input is caused by a transient increase in the conductance of the membrane to certain ions. Reprinted by permission from Brown and Johnston (1983).

pyramidal cell.[3] The figure is taken from an experiment by Brown and Johnston (1983), which demonstrated for the first time how a synapse within the central nervous system could be voltage clamped. The *voltage-clamp* technique was previously used on the very large synapse made between the axonal terminals of motoneurons and the muscle, the so-called *neuromuscular junction* (Katz, 1966; Johnston and Wu, 1995). It allows the experimentalist to stabilize the membrane potential (via a feedback loop) at some fixed value, irrespective of the currents that are flowing across the membrane in response to some stimulus. This allows the measurement of EPSCs at various fixed potentials (as in Fig. 1.6). The EPSC has its largest value at a holding potential of -65 mV, becoming progressively smaller and vanishing around 0 mV. If the membrane potential is clamped to values more positive than zero, the EPSC reverses sign (Fig. 1.6A). When the relationship between the peak current and the holding potential is plotted (Fig. 1.6B), the data tend to fall on a straight line that goes through zero around -1.9 mV and that has a slope of 20.6 nS.

What we can infer from such a plot is that the postsynaptic event is caused by a temporary increase in the membrane conductance, here by a maximal increase of about 20 nS

3. It should be pointed out that we are here looking at a population of synapses, made very close to the soma of the pyramidal cell, thereby minimizing space-clamp problems.

(due to simultaneous activation of numerous synapses) in series with a so-called *synaptic reversal battery* or potential, $E_{syn} = -1.9$ mV (since the conductance change is specific for a particular class of ions). Spiking activity in the presynaptic cell triggers, through a complicated cascade of biophysical events (further discussed in Chap. 4), a conductance change in the membrane of the postsynaptic cell. Typically, the conductance $g_{syn}(t)$ transiently increases within less than 1 msec, before this increase subsides within 5 msec. The equivalent electrical circuit diagram of a synapse embedded into a patch of neuronal membrane is shown in Fig. 1.7A. It is important to understand that from a biophysical, postsynaptic point of view, a synapse does not correspond to a fixed current source—in that case the slope of the I–V curve in Fig. 1.6 should have been zero—but to a genuine increase in the membrane conductance. As we will reemphasize throughout the book, this basic feature of the neuronal hardware has a number of important functional consequences.

Because of the existence of the synaptic battery, the *driving potential* across the synapse is the difference between E_{syn} and the membrane potential. The postsynaptic current due to a single such synapse is given by Ohm's law

$$I_{syn} = g_{syn}(t)(V_m(t) - E_{syn}) . \tag{1.18}$$

Inserting this synapse into a patch of membrane (Fig. 1.7A) gives rise to the following ordinary differential equation (on the basis of Kirchhoff's current law):

$$C\frac{dV_m}{dt} + g_{syn}(t)(V_m - E_{syn}) + \frac{V_m - V_{rest}}{R} = 0 \tag{1.19}$$

or, with $\tau = CR$, the passive membrane time constant in the absence of any synaptic input, we can transform this into

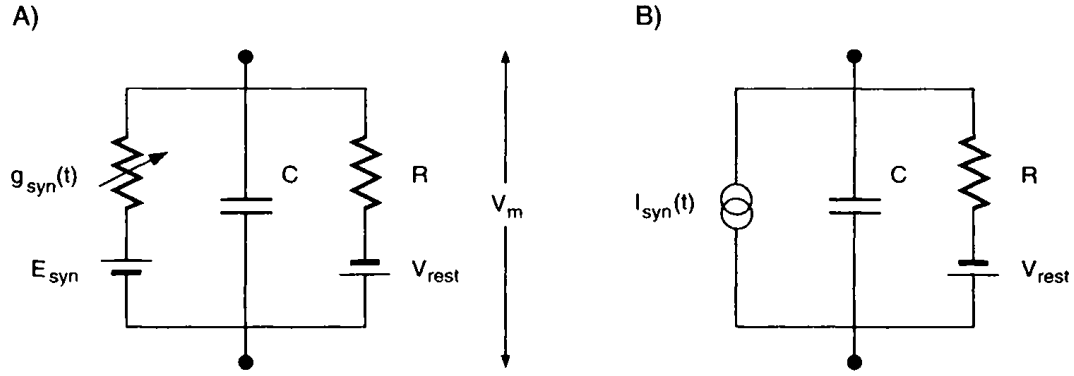

Fig. 1.7 Equivalent Electrical Circuit of a Fast Chemical Synapse **(A)** Electrical model of a fast voltage-independent chemical synapse. This circuit was put forth to explain events occurring at the neuromuscular junction by Katz (1969). Remarkably, all fast chemical synapses in the central nervous system, with the exception of the voltage-dependent NMDA receptor-synaptic complex, operate on the same principle. Activation of the synapse leads to the transient opening of ionic channels, selective to certain ions. This corresponds to a transient increase in the membrane conductance $g_{syn}(t)$ in series with the synaptic reversal potential E_{syn}, shown here in parallel with a passive membrane patch. **(B)** If the evoked potential change is small relative to the synaptic reversal potential, the synapse can be approximated by a current source of amplitude $g_{syn}(t)E_{syn}$. In general, however, this will not be the case and synaptic input must be treated as a conductance change, a fact that has important functional consequences.

$$\tau \frac{dV_m}{dt} = -(1 + Rg_{\text{syn}}(t))V_m + Rg_{\text{syn}}(t)E_{\text{syn}} + V_{\text{rest}} . \tag{1.20}$$

Frequently the time course of synaptic input is approximated by a so-called α function. It describes the transient behavior of synaptic input for a number of preparations, such as nicotinic input to vertebrate sympathetic ganglion cells or the synaptic input mediated by the mossy fibers (Brown and Johnston, 1983; Williams and Johnston, 1991; Yamada, Koch, and Adams, 1998), reasonably well:[4]

$$g_{\text{syn}}(t) = \text{const} \cdot te^{-t/t_{\text{peak}}} . \tag{1.21}$$

We can now integrate Eq. 1.20 using the same values for t_{peak} and g_{peak}, but three different values for the synaptic reversal potential (Fig. 1.8).

If $E_{\text{syn}} > V_{\text{rest}}$, the synaptic current is inward and—by convention—negative and will act to depolarize the membrane. This is the hallmark of an EPSP, as observed at the most

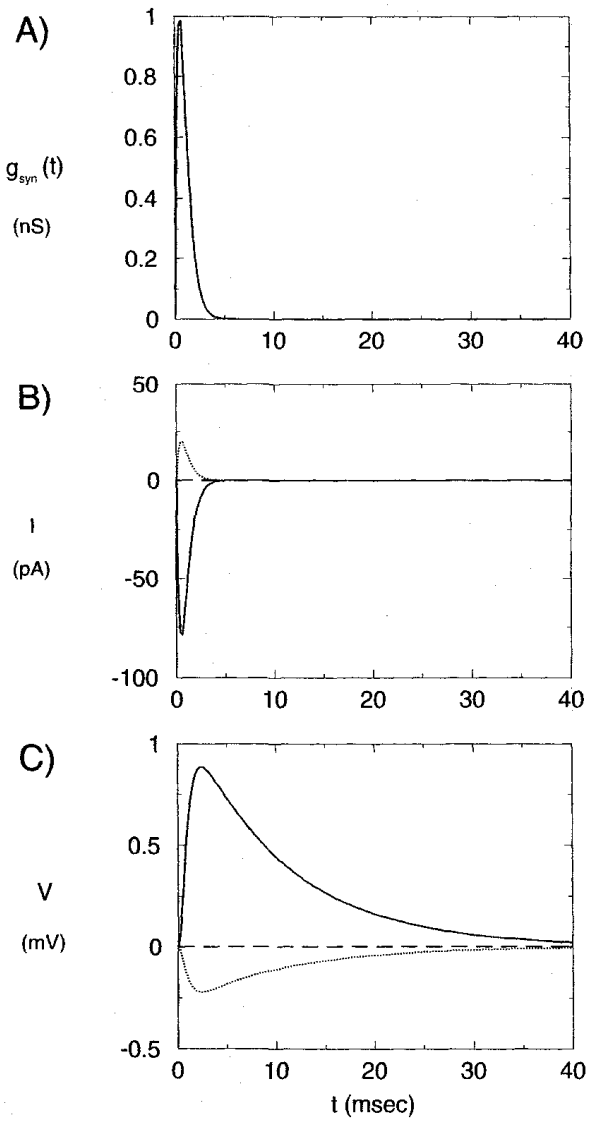

Fig. 1.8 Action of a Single Synapse Inserted into a Membrane Three different types of synaptic inputs and their differential effect on the membrane potential. **(A)** Time course of the synaptic-induced conductance increase, here with t_{peak}=0.5 msec and g_{peak} = 1 nS (Eq. 1.21). The synapse is inserted into a patch of membrane (Fig. 1.7A) with R = 100 MΩ, C = 100 pF, and τ = 10 msec. **(B)** Postsynaptic current in response to the conductance increase if the synaptic reversal potential is positive (E_{syn} = 80 mV relative to rest; solid line), negative (E_{syn} = −20 mV; dotted line), and zero (so-called shunting inhibition; dashed line). By convention, an inward current that depolarizes the cell is plotted as a negative current. **(C)** Associated EPSP (solid line) and IPSP (lower dashed line), relative to V_{rest}, solved by numerical integration of Eq. 1.20. Notice that the time course of the postsynaptic potential is much longer than the time course of the corresponding postsynaptic current due to the low-pass nature of the membrane. Shunting inhibition by itself does not give rise to any change in potential (center dashed line).

4. g_{peak}, its peak value, attained at $t = t_{\text{peak}}$, defines const = $g_{\text{peak}}\, e^1 / t_{\text{peak}}$.

common fast, excitatory synapse in the brain, the so-called non-NMDA synapse (named after its insensitivity to *N*-methyl-D-aspartic acid) that uses the neurotransmitter glutamate with a reversal potential about 80–100 mV above the resting potential of the cell (for more details, see Sec. 4.6).

If the converse occurs, that is, $E_{\text{syn}} < V_{\text{rest}}$, the current is outward and the membrane is hyperpolarized, away from the threshold for spike generation. In the central nervous system, this is typically caused by a slower form of inhibition due to γ-aminobutyric acid B receptors (GABA_B) at synapses that release the neurotransmitter GABA and that let potassium ions out of the cell and have a reversal potential 10–30 mV below the resting potential (Fig. 1.8).

What happens if a synapse is activated whose battery potential is close to the membrane potential, that is, $E_{\text{syn}} \approx V_{\text{rest}}$? If the membrane is at rest, no driving potential exists across the synaptic conductance, since $V_m - E_{\text{syn}} \approx 0$, and the membrane potential remains unperturbed. But the total conductance of the membrane increases by $g_{\text{syn}}(t)$.

If this system is now depolarized by excitatory input, activation of this *silent* or *shunting*[5] inhibition causes a reduction in the EPSP amplitude.

Activation of a GABA_A synapse, one of the most common forms of fast inhibition in cortex and associated structures, increases the membrane conductance for chloride ions and has a reversal potential in the neighborhood of many cells' resting potential, thereby implementing a form of shunting inhibition.

How do we deal with multiple synaptic inputs? Since currents add, we can extend Eq. 1.19 in a straightforward manner by placing the synapses in parallel with the *RC* circuit,

$$C\frac{dV_m}{dt} = \sum_{i=0}^{n} g_{syn,i}(t)(E_{syn,i} - V_m) + \frac{V_{\text{rest}} - V_m}{R} \tag{1.22}$$

where the sum is taken over all synapses (each of which can have its own reversal potential). Of course, this is very reminiscent of the linear summation of inputs in the "units" of standard neural network theory (see Sec. 14.4).

1.5 Synaptic Input Is Nonlinear

What is not immediately apparent from Eq. 1.22 is the fact that synaptic input as conductance change is of necessity nonlinear; that is, the change in membrane potential is a nonlinear function of the synaptic input. Yet this turns out to be crucial. From the point of view of information processing, a linear noiseless system cannot create or destroy information. Whatever information is fed into the system is available at the output. Of course, any system existing in the real world has to deal with noise, which places restrictions on the amplitude of signals that can be discriminated. Therefore in a noisy linear system, information can be destroyed. But what is needed in a system that processes information are nonlinearities that can perform discriminations and decisions. Similarly, in order for a digital system to be Turing universal, a nonlinearity such as negation and logical ANDing is required. As we will see later on, one ever-present nonlinearity is the voltage threshold for spike initiation. As we will see now, another nonlinearity that comes for free with synaptic hardware is saturation.

5. Because both excitatory and inhibitory fast synapses act to increase a postsynaptic membrane conductance, all of them can properly be said to be shunting. However, in this book we follow widespread usage and only refer to shunting inhibition as a conductance increase with a reversal potential in the neighborhood of the cell's resting potential.

1.5.1 Synaptic Input, Saturation, and the Membrane Time Constant

The nature of this effect can be perfectly well understood for a single synaptic input. If we consider the change in membrane potential relative to rest in response to a slowly varying synaptic input (that is, we can reduce $g_{\text{syn}}(t)$ to g_{syn}), we can express the dynamics of V as

$$\tau' \frac{dV}{dt} = -V + \frac{g_{\text{syn}} E_{\text{syn}}}{G_{\text{in}}} \tag{1.23}$$

where the new value of the input conductance is

$$G_{\text{in}} = g_{\text{syn}} + \frac{1}{R} \tag{1.24}$$

and the new value of the time constant in the presence of synaptic input is

$$\tau' = \frac{C}{G_{\text{in}}} = \frac{RC}{1 + Rg_{\text{syn}}} . \tag{1.25}$$

In other words, each synaptic input, whether excitatory, shunting, or inhibitory, increases the synaptic input conductance, thereby decreasing the membrane time constant (Fig. 1.9). This is, of course, equally true when one considers the effect of numerous simultaneous synaptic inputs. As we shall see further along in this book, under physiological conditions neurons can be bombarded with massive synaptic input, which will lower the membrane time constant significantly, as compared to the value of τ measured under slice conditions in the absence of normal synaptic input.

How does the membrane potential behave as a function of g_{syn}? Solving for Eq. 1.23 yields for the steady-state potential

$$V_\infty = \frac{Rg_{\text{syn}} E_{\text{syn}}}{1 + Rg_{\text{syn}}} . \tag{1.26}$$

If the synaptic input is small, that is, if $Rg_{\text{syn}} \ll 1$ or $g_{\text{syn}} \ll 1/R$, the denominator is roughly equal to 1, and the EPSP is

$$V \approx Rg_{\text{syn}} E_{\text{syn}} . \tag{1.27}$$

Here, the input can be approximated to a fair degree by a constant current source of amplitude $g_{\text{syn}} E_{\text{syn}}$. Doubling the input under these conditions leads to a doubling of the voltage change.

As the EPSP becomes larger and larger, the driving potential across the synaptic conductance $V_m - E_{\text{syn}}$ becomes smaller and smaller, disappearing eventually at $V_m = E_{\text{syn}}$. No matter how large the conductance increase is made, there is no more potential to drive ions across the membrane. Here, $Rg_{\text{syn}} \gg 1$ (or equivalently, $g_{\text{syn}} \gg 1/R$; that is, the synaptic input is considerably larger than the input conductance), and we have

$$V \approx \frac{Rg_{\text{syn}} E_{\text{syn}}}{Rg_{\text{syn}}} = E_{\text{syn}} . \tag{1.28}$$

The membrane potential has saturated at the synaptic reversal potential (Fig. 1.9).

1.5.2 Synaptic Interactions among Excitation and Shunting Inhibition

As we are devoting the entire Chap. 5 to the topic of synaptic interaction, we focus here on the specific interaction between excitatory input and shunting inhibition occurring within a single RC compartment (Fig. 1.10A). For the sake of simplicity, we assume that at $t = 0$, both excitation (of constant amplitude g_e and battery E_e) and shunting inhibition (of constant

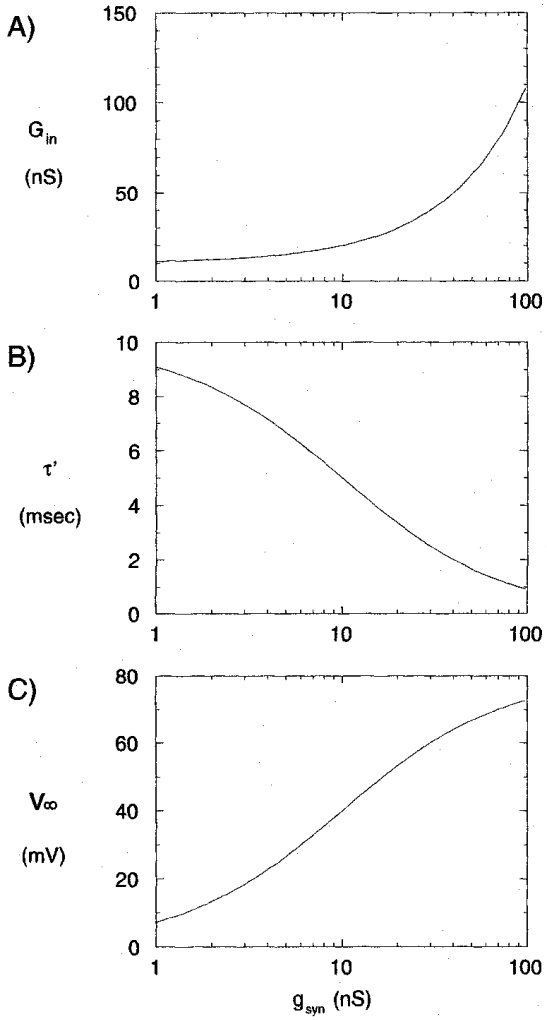

Fig. 1.9 Synaptic Input, Saturation, and the Time Constant The effect of varying the synaptic input conductance on **(A)** the input conductance G_{in} (Eq. 1.24), **(B)** the membrane time constant τ' (Eq. 1.25), and **(C)** the steady-state change in membrane potential V_{∞} (Eq. 1.26) in a single-compartment model (Fig. 1.7A) as a function of g_{syn}. Conceptually, if we assume an excitatory synapse (with $E_{\text{syn}} = 80$ mV) and a fixed peak amplitude of $g_e = 1$ nS, the x axis is logarithmic in the number of synapses involved in the overall synaptic event. Note that τ' as well as G_{in} will increase irrespective of whether the synapses are depolarizing, shunting, or hyperpolarizing. The fact that the input to neurons comes in the form of a change in the membrane conductance implies that the very structure of the neuronal hardware changes with the input, since the dynamics of the cell speeds up in the presence of strong synaptic input.

amplitude g_i and battery $E_i = V_{\text{rest}}$) are turned on and remain on. Using Kirchhoff's current law, we can express the change in membrane potential relative to V_{rest} in this circuit as

$$C\frac{dV}{dt} = g_e(E_e - V) - g_i V - \frac{V}{R}. \tag{1.29}$$

As in Eq. 1.23, we can transform this into

$$\tau'\frac{dV}{dt} = -V + \frac{g_e E_e}{G_{\text{in}}} \tag{1.30}$$

where the input conductance in the presence of the two synaptic inputs is

$$G_{\text{in}} = g_e + g_i + \frac{1}{R} \tag{1.31}$$

and the time constant is

$$\tau' = \frac{C}{G_{\text{in}}}. \tag{1.32}$$

The solution to this is a low-pass filter function multiplied with some constant, or

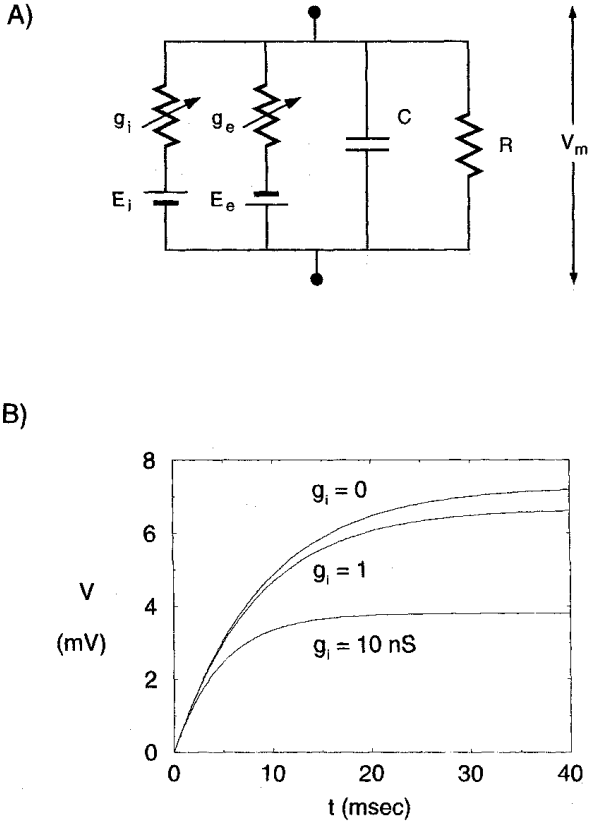

Fig. 1.10 NONLINEAR INTERACTION BETWEEN EXCITATION AND SHUNTING INHIBITION Inhibitory synaptic input of the shunting type, that is, whose reversal potential is close to the cell's resting potential, can implement a form of division. **(A)** This is demonstrated for an *RC* circuit ($R = 100\,\mathrm{M\Omega}$, $C = 100\,\mathrm{pF}$) in the presence of both excitation (with battery $E_e = 80$ mV) and shunting inhibition (with $E_i = 0$). We are here only considering the change in membrane potential relative to V_{rest}. **(B)** Time course of the membrane depolarization in response to a step onset of both excitation (of amplitude $g_e = 1$ nS) and shunting inhibition (for three values of $g_i = 0$, 1, and 10 nS). One effect of increasing g_i is an almost proportional reduction in EPSP amplitude. A further consequence of increasing the amount of shunting inhibition is to decrease the time constant τ', from its original 10 msec in the absence of any synaptic input to 9 msec in the presence of only excitation to 4.8 msec in the presence of excitation and the 10 times larger shunting inhibition.

$$V(t) = \frac{g_e E_e}{G_{\mathrm{in}}}(1 - e^{-t/\tau'}) . \tag{1.33}$$

(This can be checked by replacement into Eq. 1.30.) The steady-state potential for $t \to \infty$ converges to

$$V_\infty = \frac{g_e R E_e}{1 + g_e R + g_i R} . \tag{1.34}$$

What is important to realize is that the numerator does not include any contribution from the shunting inhibition (since the synaptic reversal potential is equal to the resting potential); g_i only appears in the denominator. Increasing g_i therefore reduces the EPSP from its peak value in a *division*-like manner. This is the reason shunting inhibition is frequently also referred to as *divisive inhibition* (Bloomfield, 1974; Torre and Poggio, 1978). Of course, due to the offset in the denominator, g_i only implements a true division in the limit of $g_i \gg g_e + 1/R$. Under these conditions,

$$V_\infty \approx \frac{g_e E_e}{g_i} . \tag{1.35}$$

Increasing g_i also affects the speed with which the cell converges to its steady-state, since the time constant decreases with increasing shunting inhibition, as illustrated in Fig. 1.10B.

Finally, let us consider the *voltage gain*, that is, the sensitivity of the output to variations in the excitatory input: by how much does the amplitude of the EPSP vary if g_e varies? This amounts to computing

$$\frac{dV_\infty}{dg_e} = \frac{RE_e(1 + g_i R)}{(1 + g_e R + g_i R)^2}. \tag{1.36}$$

We see that the gain is maximal in the absence of any shunting inhibition, becoming progressively smaller as g_i increases. In the limit of $g_i \to \infty$, the gain becomes zero; in the presence of massive amounts of inhibition, the excitatory input becomes swamped and is completely dominated by inhibition.

1.5.3 Gain Normalization in Visual Cortex and Synaptic Input

One example demonstrating the use of synaptic conductance changes to implement a nonlinear operation crucial to the behavior of neurons in visual cortex has been proposed by Carandini and Heeger (1994).

The standard model of a simple cell in primary visual cortex (V1) is that its firing rate is a linear function of the visual input, using a Gabor filter for its spatial receptive field and some low-pass or band-pass filter to account for its temporal behavior (Wandell, 1995). While much evidence has accumulated in favor of this position, many V1 neurons do show a number of nonlinearities: (1) the response saturates with increasing visual contrast, (2) at higher contrast level, the response occurs earlier, and (3) superposition does not hold; that is, the response of the cell to a bar at its optimal orientation superimposed onto a bar orthogonal to its optimal orientation is not equal to the sum of the response to the two bars when presented by themselves. Carandini and Heeger (see also Nelson, 1994) account for this behavior by using a simple *RC* model for a V1 cell, as in Fig. 1.10A, augmented by an input from a hyperpolarizing synapse. Their intriguing idea is to have the amplitude of the shunting inhibition depend on the response rate of the entire population of cells at this particular location in space, summed over all orientations and direction of motions (Fig. 1.11). At high contrasts when g_e is large, the network is very active and g_i is also very large; this leads to the divisive normalization witnessed in Fig. 1.10B as well as to a reduction in the time constant, explaining the advance of the response at high contrast levels. Heeger, Simoncelli, and Movshon (1996) have argued that the very same normalization mechanism is also operating in other cortical areas. Note that a more physiological implementation of this idea needs to take the additional conductance due to massive, excitatory recurrent feedback among cortical cells into account (Ahmed et al., 1994; Douglas et al., 1995).

While the Carandini and Heeger (1994) model is elegant, leads to a simple mathematical model of a cortical cell, and can account for much of the data (Fig. 1.11), it does have one serious flaw that we can only allude to here. As will become apparent in Sec. 18.5 (Kernell, 1969, 1971; Holt and Koch, 1997), shunting inhibition acts in a linear, subtractive manner when treated within the context of a spiking neuron, rather than in the saturating manner we are accustomed to from a passive membrane. This is a natural consequence of the biophysics of spike generation and throws doubt onto the hypothesis that contrast normalization is implemented using the natural properties of conductance-increasing synapses.

1.6 Recapitulation

In this introductory chapter, we meet some of the key actors underlying neuronal information processing. Basic to all cells is the capacitance inherent in the bilipid layer, limiting how quickly the membrane potential can respond to a fixed input current. The simplest of all neuronal models is that of a single compartment that includes a resistance, in series with a

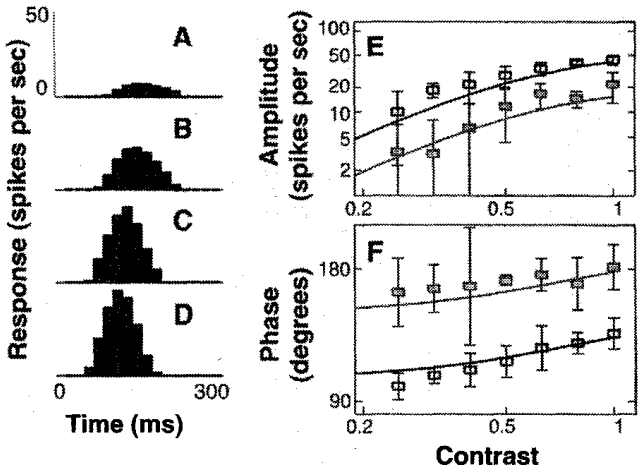

Fig. 1.11 GAIN NORMALIZATION IN NEURONS IN VISUAL CORTEX Response properties of a simple cell in primary visual cortex of the monkey in response to drifting sinusoidal gratings (Carandini and Heeger, 1994). **(A)** through **(D)** One cycle of the response to gratings of contrast 0.125, 0.25, 0.5, and 1.0. The cell saturates with contrast (doubling the contrast doubles the neuronal response when going from **A** to **B**, but not when going from **C** to **D**) and advances its response (a shift of about 50 msec occurs between **A** and **D**). **(E)** Amplitude and **(F)** Phase of the fundamental Fourier component to sinusoidal gratings drifting at 6 Hz. Shown are the responses of the cell at its preferred orientation (open symbols) and 20° away from the preferred orientation (solid symbols). Error bars represent ± 1 standard deviation and the solid lines correspond to the best fit of the model equation that uses shunting inhibition, activated via massive feedback, to carry out this gain normalization. Reprinted by permission from Carandini and Heeger (1994).

battery, and the capacitance. It can be completely described by a linear, low-pass filter. As we will see in a later chapter, such an *RC* circuit, augmented by a simple voltage threshold, constitutes one of the simplest yet also most powerful models of a spiking neuron: the *leaky integrate-and-fire unit.*

We introduced fast chemical synapses, the stuff out of which computations arise. Chemical synapses convert the presynaptic voltage signal—via a chemical process—into a postsynaptic electrical signal, via a change in the membrane conductance specific to certain ions. Such a synapse can be described by a time-dependent synaptic conductance $g_{\text{syn}}(t)$ and a synaptic battery E_{syn}. In general, synapses cannot be treated as constant current sources.

Chemical synapses, similar to an operational amplifier wired up as a follower, isolate the electrical properties of the postsynaptic site from the presynaptic one. This allows synapses to link neurons with very different electrical impedances. Furthermore, the amplitude, duration, and sign of the postsynaptic signal can be quite different from those of the presynaptic one. Electrical synapses, discussed in Sec. 4.10, share none of these properties.

The fact that synapses act by changing, usually increasing, the postsynaptic membrane conductance has a number of important consequences. It allows for the natural expression of several nonlinear operations, in particular saturation and gain normalization. As an example, we saw how shunting inhibition, mediated by a type of synapse whose synaptic reversal potential is close to the cell's resting potential, acts similar to division. We also studied how synaptic input that increases the postsynaptic membrane conductance for some combinations of ions, no matter what its reversal potential, acts to decrease the cell's input resistance and thus its membrane time constant. As postulated by Carandini and Heeger (1994), the effect of massive feedback synaptic input might, in a very physiological manner, implement *gain normalization* in cortical areas.

2

LINEAR CABLE THEORY

In the previous chapter, we briefly met some of the key actors of this book. In particular, we introduced the *RC* model of a patch of neuronal membrane and showed an instance where such a "trivial" model accounts reasonably well for the input-output properties of a neuron, as measured at its cell body (Fig. 1.4). However, almost none of the excitatory synapses are made onto the cell body, contacting instead the very extensive dendritic arbor. As we will discuss in detail in Chap. 3 (see Fig. 3.1), dendritic trees can be quite large, containing up to 98% of the entire neuronal surface area. We therefore need to understand the behavior of these extended systems having a cablelike structure (Fig. 2.1).

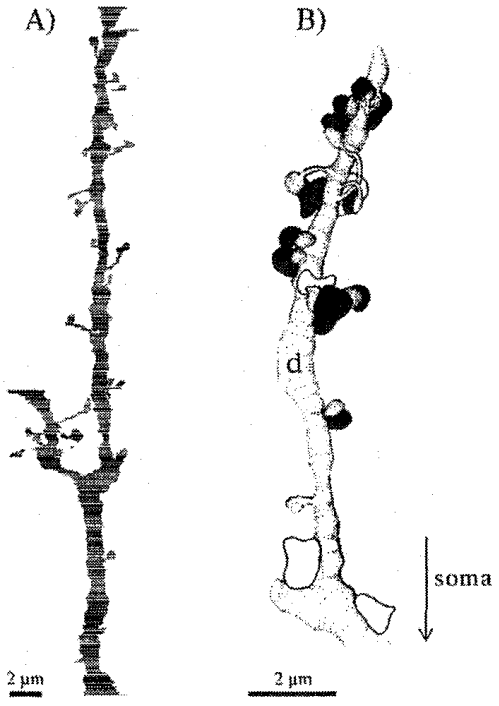

Fig. 2.1 CLOSEUP VIEW OF DENDRITES Two reconstructed dendrites of a spiny stellate cell in the visual cortex of the cat. The reconstructions were carried out by a very laborious serial electron microscopic procedure. Notice the thin elongated, thornlike structures, *dendritic spines*. The vast majority of neuronal processes, whether axons or dendrites, possess such an elongated, cylindrical geometry. Studying the spread of electrical current in these structures is the subject of cable theory. **(A)** Cross section of a branching dendrite. **(B)** Three-dimensional view of another dendrite. The black blobs are excitatory synapses and the three clear blobs are inhibitory synapses. Reprinted by permission from Anderson et al. (1994).

The basic equation governing the dynamics of the membrane potential in thin and elongated neuronal processes, such as axons or dendrites, is the *cable equation*. It originated in the middle of the last century in the context of calculations carried out by Lord Kelvin, who described the spread of potential along the submarine telegraph cable linking Great Britain and America. Around the turn of the century, Herman and others formulated the concept of *Kernleitermodel*, or core conductor model, to understand the flow of current in nerve axons. Such a core conductor can be visualized as a thin membrane or sheath surrounding a cylindrical and electrically conducting core of constant cross section placed in a solution of electrolytes (see Fig. 2.2).

The study of the partial differential equations describing the evolution of the electrical potential in these structures gave rise to a body of theoretical knowledge termed *cable theory*. In the 1930s and 1940s concepts from cable theory were being applied to axonal fibers, in particular to the giant axon of the squid (Hodgkin and Rushton, 1946; Davis and Lorente de No, 1947).[1] The application of cable theory to passive, spatially extended dendrites started in the late 1950s and blossomed in the 1960s and 1970s, primarily due to the work of Rall (1989). In an appropriate gesture acknowledging his role in the genesis of quantitative modeling of single neurons, Segev, Rinzel, and Shepherd (1995) edited an annotated collection of his papers, to which we refer the interested reader. It also contains personal recollections from many of Rall's colleagues as well as historical accounts of the early history of this field.

We restrict ourselves in this chapter to studying *linear cable theory*, involving neuronal processes that only contain voltage-independent components. In particular, we assume that the membrane can be adequately described by resistances and capacitances (*passive membrane*). Given the widespread existence of dendritic nonlinearities, it could be argued that studying neurons under such constraints will fail to reveal their true nature. However, it is also true that one cannot run before one can walk, and one cannot walk before one can crawl. In order to understand the subtlety of massive synaptic input in spatially extended passive and active cables, one first needs to study the concepts and limitations of linear cable theory before advancing to nonlinear phenomena.

Cable theory, whether linear or nonlinear, is based on a number of assumptions concerning the nature and geometry of neuronal tissue. Let us discuss these assumptions prior to studying the behavior of the membrane potential in a single, unbranched, passive cable.

2.1 Basic Assumptions Underlying One-Dimensional Cable Theory

In a standard copper wire, electrons drift along the gradient of the electrical potential. In axons or dendrites the charge carriers are not electrons but, in the main, one of two ionic species, sodium and potassium, and, to a lesser extent, calcium and chloride. How can this current be quantified?

1. Starting point for any complete description of electrical currents and fields must be Maxwell's equations governing the dynamics of the electric field $\mathbf{E}(x, y, z, t)$ and the magnetic field $\mathbf{B}(x, y, z, t)$,[2] supplemented by the principle of conservation of charge

1. For a detailed account of all the twists and turns of this story, see Cole (1972) and Hodgkin (1976). When reading these down-to-earth monographs, one becomes painfully aware of the very limited amount of real knowledge and insight gained during decades of intensive experimental and theoretical research. Most of one's effort is usually spent on pursuing details that turn out to be irrelevant and in constructing and developing incorrect models.

2. We follow standard convention in using boldface variables for all vector quantities.

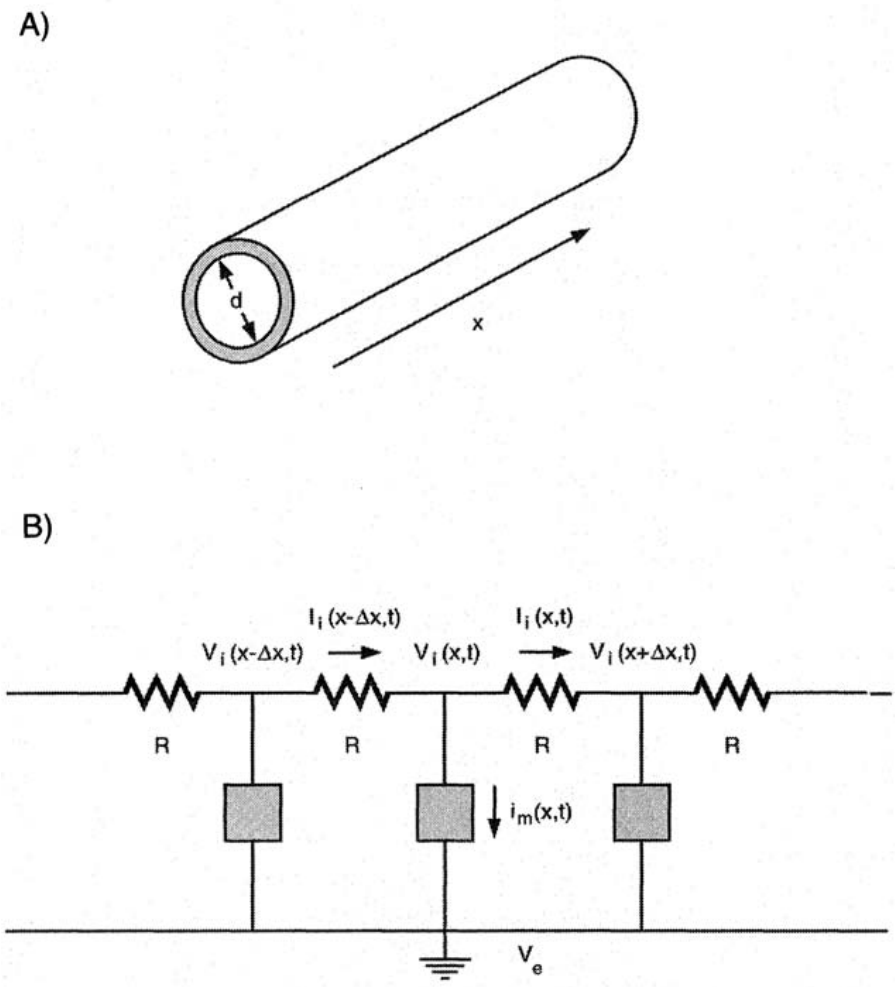

Fig. 2.2 Electrical Structure of a Cable **(A)** Idealized cylindrical axon or dendrite at the heart of one-dimensional cable theory. Almost all of the current inside the cylinder is longitudional due to geometrical (the radius is much smaller than the length of the cable) and electrical factors (the membrane covering the axon or dendrite possesses a very high resistivity compared to the intracellular cytoplasm). As a consequence, the radial and angular components of the current can be neglected, and the problem of determining the potential in these structures can be reduced from three spatial dimensions to a single one. On the basis of the bidomain approximation, gradients in the extracellular potentials are neglected and the cable problem is expressed in terms of the transmembrane potential $V_m(x, t) = V_i(x, t) - V_e$. **(B)** Equivalent electrical structure of an arbitrary neuronal process. The intracellular cytoplasm is modeled by the purely ohmic resistance R. This tacitly assumes that movement of carriers is exclusively due to drift along the voltage gradient and not to diffusion. Here and in the following the extracellular resistance is assumed to be negligible and V_e is set to zero. The current per unit length across the membrane, whether it is passive or contains voltage-dependent elements, is described by i_m and the system is characterized by the second-order differential equation, Eq. 2.5.

(Feynman, Leighton, and Sands, 1964). As detailed in Rosenfalck's thesis (1969), the magnetic vector potential associated with the movement of charges during an action potential in biological tissues only has a negligible effect (10^{-9}) on the electric field and can therefore safely be neglected. Indeed, it took the technological development of very sensitive quantum devices (SQUIDs) to be able to measure the magnetic field associated with massive electrical activity in the brain. So the first simplification involves neglecting the magnetic field.

2. This leaves us with three fundamental relationships governing electrodynamics in neuronal structures.

   a. Gauss's law, stating that the divergence of the field **E** is identical to the charge density normalized by the electrical permittivity ϵ. Equivalently, Poisson's equation, which links the Laplacian of the electrical potential to the negative charge density normalized by ϵ, serves as well.

   b. Charge conservation, that is, the sum of the flux of current through any closed surface and the change of the charge over time inside this surface must be zero.

   c. An equation linking the electrical current to the electric field. In general, charged carriers can move either by drift along an electric field or by diffusion, from a volume of high carrier concentration into one of lower concentration, and the total current flow is the sum of these two independent components. The mathematical expression of this fact constitutes the Nernst-Planck electrodiffusion equation, treated in Sec. 11.3. As discussed there, for almost all cases of interest the changes in concentration of the various ions (Na^+, K^+, Ca^{2+} and Cl^-) are too small to measurably contribute to current flow. Only in very thin fibers of less than 1 μm diameter does longitudinal current flow due to concentration differences begin to play any role. In other words, Ohm's law is perfectly adequate to describe the electrical current moving within an axon or dendrite.[3]

3. This is the starting point for most derivations of cable theory (Lorente de Nó, 1947; Clark and Plonsey, 1966, 1968; Plonsey, 1969; Rall, 1969b; Eisenberg and Johnson, 1970).

   a. The dominant fraction of current inside a neuronal process, such as a dendrite or axon, flows parallel to its longitudinal axis. Only a very small fraction of the current flows across the neuronal membrane. This is true both for geometrical reasons—the diameter of axons and dendrites being much smaller than their longitudinal extent—as well as for electrical ones. As detailed in Appendix A, the neuronal membrane is all but impermeable to current flow. Charged carriers can only cross the membrane through the ionic channels. The high transmembrane resisitivity stands in contrast to the relatively small intracellular resistivity.

   A major implication is that instead of having to solve for the voltage in three dimensions, our problem is reduced to one of describing the voltage along a single spatial dimension. In a careful comparison between the membrane potential derived as the solution of Laplace's equation in a three-dimensional cylindrical coordinate system and the solution of the one-dimensional cable equation, Rall (1969b) showed that the radial and angular membrane potential terms typically decay 10^4 times faster than the components of the membrane potential along the axis. Fortuitously, we can safely neglect two out of three dimensions for all of the cases considered in this book.

   b. Electrical charge in the cytoplasm, no matter whether inside or outside the cell, relaxes in a matter of microseconds or less. In other words, any capacitive effects of the cytoplasm itself can be totally ignored on the millisecond or longer time scale (inductive effects can be completely neglected; Scott, 1971). Thus, from an electrical point of view, the extracellular as well as the intracellular cytoplasm can be approximated by ohmic resistances.

---

3. This is analogous to the situation prevalent in a copper wire, where the current flow due to drift down the gradient of the electrical potential exceeds by many orders of magnitude the current flow due to differences in the local densities of electrons.

c. The solution of the equation for the electrical potential is still extremely complicated if all the neuronal structures and membranes outside the dendrite or axon under investigation are explicitly included. Fortuitously for modelers (but less so for the electrophysiologist, who has to infer the neuronal activity of a cell from its extracellular signature), the extracellular potential (1) usually is small (since the small amount of current making it through the membrane encounters a relatively large extracellular volume), and (2) decays over distances which are usually much larger than the diameters of the fiber itself. This implies that the extracellular space can be treated as a homogeneous dielectric, averaging over local inhomogeneities. The problem of computing the membrane potential is therefore reduced to two homogeneous domains, the extracellular and the intracellular ones.

The extracellular resistivity is often defined in the case when the external medium is a shell of conducting cytoplasm surrounding the cable, a shell that can be characterized by a resistance per unit length of cylinder r_e. For large external volumes (think of the case of a single neuronal fiber placed in a bath solution) r_e is assumed to be zero. In this case, no extracellular voltage gradients exist and the entire extracellular space is isopotential, $V_e(x, t) = \text{const}$, which we set to zero. Including a uniform extracellular resistivity complicates matters only slightly, and the solution of the cable equation is qualitatively similar to the solution for $r_e = 0$. Therefore, the *membrane potential* $V_m(x, t)$, defined as the intracellular potential minus the extracellular potential (Eq. 1.1), is identical to the intracellular potential. Indeed, throughout the book, we use these two variables interchangeably. Yet it should always be kept in mind that the membrane potential corresponds to the difference in voltage across the membrane separating the inside from the outside.

A timely research topic of considerable interest is a detailed investigation of electrical coupling of realistically modeled neurons via the extracellular potential. Lengthy experimental and theoretical studies have been carried out for the case of two parallel axons. For this geometry, any direct electrical coupling is slight (the extracellular potential due to a spike is in the 10 μV range; Clark and Plonsey, 1968, 1971; Marks and Loeb, 1976; Scott and Luzader, 1979; Barr and Plonsey, 1992; Bose and Jones, 1995; Struijk, 1997). However, extracellular potentials recorded close to dendritic trees can be much larger (up to a few mV) than those next to axons. Given the extremely tight packing among neurons, this type of ephaptic[4] coupling could be of functional relevance, yet almost no theoretical work has been carried out on this subject (Lorente de Nó, 1953; Hubbard, Llinás and Quastel, 1969; Holt, 1998).

At this stage, we represent the neuronal tissue with the help of a series of discrete electrical circuits of the type shown in Fig. 2.2B. Without making any specific assumption concerning the detailed nature of the neuronal membrane, we express the current per unit length flowing through the membrane at location x as $i_m(x, t)$. We can write down Ohm's law for the discrete circuit illustrated in Fig. 2.2B,

$$V_i(x, t) - V_i(x + \Delta x, t) = R I_i(x, t) \tag{2.1}$$

or, in the limit of an infinitesimal small interval Δx, and with $V_m = V_i$,

$$\frac{\partial V_m}{\partial x}(x, t) = -r_a \cdot I_i(x, t)\,, \tag{2.2}$$

4. Greek for "touching onto," rather than *synaptic*, "touching together."

where $r_a = R/\Delta x$ is the intracellular resistance per unit length of cable with dimensions of ohms per centimeter. I_i is the intracellular core current flowing along the cable, assumed to be positive when flowing toward the right, in the direction of increasing values of x. Kirchhoff's law of current conservation stipulates that the sum of all currents flowing into and out of any particular node must equal zero. Applied to the node at x in Fig. 2.2B, we have

$$i_m(x,t)\Delta x + I_i(x,t) - I_i(x-\Delta x,t) = 0 \tag{2.3}$$

or, in differential form in the limit that $\Delta x \to 0$,

$$i_m(x,t) = -\frac{\partial I_i}{\partial x}(x,t)\,. \tag{2.4}$$

Inserting the spatial derivative of Eq. 2.2 into Eq. 2.4 leads to

$$\frac{1}{r_a}\frac{\partial^2 V_m}{\partial x^2}(x,t) = i_m(x,t)\,. \tag{2.5}$$

This second-order ordinary differential equation, together with appropriate boundary conditions, describes the membrane potential in an extended one-dimensional cable structure with an ohmic intracellular cytoplasm, regardless of the exact nature of the neuronal membrane.

2.1.1 Linear Cable Equation

In Sec. 1.1, we discussed the nature of a patch of passive membrane and assumed that the membrane current includes a capacitive (Eq. 1.3) and a resistive (Eq. 1.4) component (Figs. 1.1 and 1.2). Including an external current term $I_{\text{inj}}(x,t)$, the membrane current per unit length of the cable, i_m, is given by

$$i_m(x,t) = \frac{V_m(x,t) - V_{\text{rest}}}{r_m} + c_m\frac{\partial V_m(x,t)}{\partial t} - I_{\text{inj}}(x,t)\,, \tag{2.6}$$

where r_m is the membrane resistance of a unit length of fiber, measured in units of ohms-centimeter. If the electrical nature of the membrane is constant along the length of the passive fiber under investigation (Fig. 2.3), we can replace $i_m(x,t)$ on the right-hand side of Eq. 2.5 with Eq. 2.6 and multiply both sides with r_m to arrive at

$$\lambda^2\frac{\partial^2 V_m(x,t)}{\partial x^2} = \tau_m\frac{\partial V_m(x,t)}{\partial t} + (V_m(x,t) - V_{\text{rest}}) - r_m I_{\text{inj}}(x,t)\,, \tag{2.7}$$

with the membrane time constant $\tau_m = r_m c_m$ and the *steady-state space constant* $\lambda = (r_m/r_a)^{1/2}$. We will discuss their significance forthwith.

Equation 2.7 is the *linear cable equation*, a partial differential equation, first order in time and second order in space. This type of parabolic differential equation is quite similar to the heat and diffusion equations. The behavior of all three is characterized by dissipation and the absence of any wavelike solution with constant velocity. Parabolic differential equations have a well-specified and unique solution if appropriate initial conditions, such as the voltage throughout the cable at $t = 0$ should be zero, or boundary conditions, such as no current should leak out at either end of the cable, are specified. The cable equation is fundamental to understanding the behavior of the membrane potential, the principal state variable used for rapid intracellular communication in neurons. We will discuss its behavior in both this chapter and the next.

As expressed in Eq. 2.7, a simple, unbranched cable has a nonzero resting potential V_{rest} which does not vary with the position along the cable. For a homogeneous cable in the

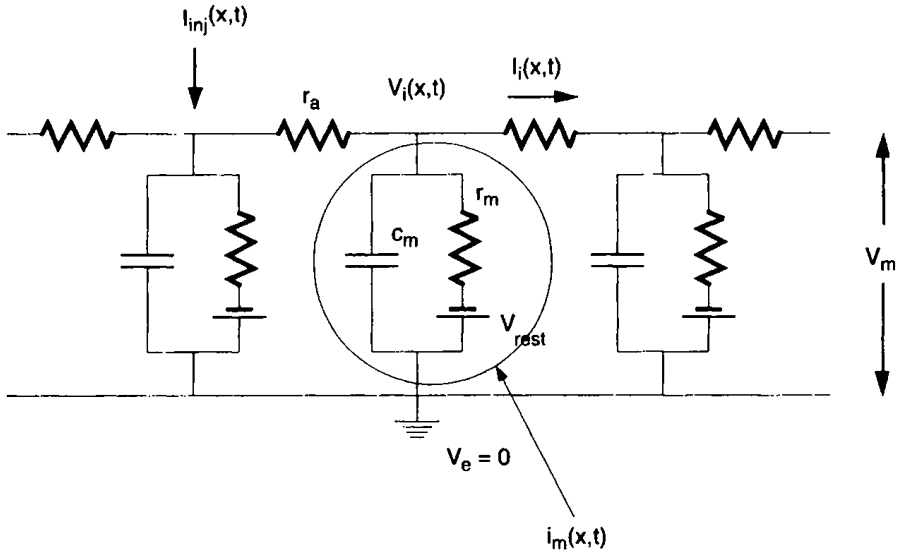

Fig. 2.3 A Single Passive Cable Equivalent lumped electrical circuit of an elongated neuronal fiber with passive membrane. The intracellular cytoplasm is described by an ohmic resistance per unit length r_a and the membrane by a capacitance c_m in parallel with a passive membrane resistance r_m and a battery V_{rest}. The latter two components are frequently referred to as *leak resistance* and *leak battery*. An external current $I_{inj}(x,t)$ is injected into the cable. The associated linear cable equation (Eq. 2.7) describes the dynamics of the electrical potential $V_m = V_i - V_e$ along the cable.

absence of any input $I_{inj}(x,t)$, the membrane potential throughout the cable will be equal to a constant. The amplitude of V_{rest} varies between -50 and -90 mV, depending on cell type and other circumstances, with the inside of the neuron being at the negative potential. V_{rest} need not always be constant throughout the dendritic tree (see Sec. 18.3.4).

Because the resting potential is simply an offset, it is often set to zero. This can be thought of as defining the membrane potential $V_m(x,t)$ as relative to this resting potential. Very often the equations will be somewhat simplified when the potential is defined as relative to V_{rest}. We use the convention that $V_m(x,t)$ refers to the absolute membrane potential, while $V(x,t)$ refers to the potential relative to V_{rest}.

We should here also allude to the vexing question of units. The three voltage-independent components of a passive cable are commonly specified in one of two ways. If they are expressed as quantities per unit length, they are conventionally labeled

$$r_a = \frac{4R_i}{\pi d^2} \tag{2.8}$$

in units of Ω/cm,

$$r_m = \frac{R_m}{\pi d} \tag{2.9}$$

in units of Ω·cm and

$$c_m = C_m \cdot \pi d \tag{2.10}$$

in units of F/cm. Using these variables has the advantage that the cable equation contains no explicit terms depending on the diameter d of the cable.

The more common way, and the one we adopt throughout the book, is to specify these quantities in units that are independent of the diameter of the fiber, using capital letters: the

intracellular resistivity R_i, the *specific membrane resistance* R_m and the *specific membrane capacitance* C_m, with dimensions of Ω·cm, $\Omega \cdot \text{cm}^2$ and F/cm^2, respectively. For more details, consult Appendix A.

2.2 Steady-State Solutions

Let us investigate the behavior of the cable equation in response to a current $I_{\text{inj}}(x)$ injected at location x via an intracellular microelectrode or a synapse. We assume that the current is switched on at $t = 0$ and remains on. One frequently encounters this situation in experiments to investigate the cable properties of neurons and axons. After some initial transients, the voltage will reach a steady-state value. To compute the steady-state membrane potential, we set $\partial V/\partial t = 0$ and write the cable equation as

$$\lambda^2 \frac{d^2V(x)}{dx^2} = V(x) - r_m I_{\text{inj}}(x) . \tag{2.11}$$

This reduces the original partial differential Eq. 2.7 to an ordinary second-order differential equation depending solely on space. We now study its solutions for different neuronal geometries.

2.2.1 Infinite Cable

We begin by assuming that a current I_{inj} of constant amplitude is injected at the origin, $x = 0$, of an infinite cable of diameter d. Mathematically, we describe this by setting $I_{\text{inj}}(x)$ to $I_0\delta(x)$, where $\delta(x)$ is the Dirac *delta* or *impulse* distribution in space. As boundary condition we assume that the voltage at the two infinitely distant terminals goes to zero as $|x| \to \infty$. Using the theory of Fourier transforms (see Appendix B) we arrive at the solution

$$V(x) = V_0 e^{-|x|/\lambda} , \tag{2.12}$$

with $V_0 = I_0 r_m/(2\lambda)$. This solution can easily be verified by placing it into Eq. 2.11. The stationary voltage distribution, sometimes referred to as the *electrotonus*, in the infinite cable decays exponentially away from the site of injection. The parameter controlling this decay is the *space constant* λ. The voltage decreases to e^{-1}, that is, to 37% of its original value, at $x = \lambda$ and to e^{-2}, or 13% of its original value, at $x = 2\lambda$. In the derivation of the cable equation, the *steady-state space constant* is defined as

$$\lambda = \left(\frac{r_m}{r_a}\right)^{1/2} = \left(\frac{R_m}{R_i} \cdot \frac{d}{4}\right)^{1/2} . \tag{2.13}$$

The larger the membrane resistance R_m, the less current leaks across the membrane and the larger the space constant λ. Furthermore, a thick dendrite has a larger space constant than a thin one, reflecting the fact that the spread of current is enhanced by a larger diameter. Another way of deriving λ involves computing the distance l over which the total resistance to current flowing across the membrane is identical to the total longitudinal resistance. Paying careful attention to the relevant units, we have $r_m/l = r_a l$, or $l = \sqrt{r_m/r_a} = \lambda$. For a typical apical dendrite of a cortical cell with a 4 μm diameter, $R_i = 200$ Ω·cm and $R_m = 20,000\ \Omega \cdot \text{cm}^2$, the space constant λ comes out to be 1 mm. This large distance, compared to the diameter of the dendrite, is the reason why we can neglect the radial components of voltage along these cables.

Given the importance of λ for the electrotonic spread of the potential in a neuron, we frequently normalize the spatial coordinate x with respect to λ, expressing it in dimensionless units: $X = x/\lambda$. Any particular distance ℓ can likewise be expressed in terms of the associated dimensionless *electrotonic distance* $L = \ell/\lambda$.

What is the input resistance of the infinite cable? Operationally, it is measured by inserting an electrode that passes current and, at a distance that is small compared to λ, an electrode to record the voltage. In the limit that this distance shrinks to zero, we can write

$$R_{\text{in}} = \frac{V(x)}{I_i(x)} = \frac{V(x=0)}{I_0}. \tag{2.14}$$

The last equality holds because the input resistance at the location of the injecting electrode is, by definition, equal to the ratio of the evoked potential to the injected current causing this change. It follows that

$$R_{\text{in}} = \frac{r_m}{2\lambda} = \frac{r_a\lambda}{2} = \frac{(r_a r_m)^{1/2}}{2}. \tag{2.15}$$

The input resistance is—as expected—constant throughout the infinite and homogeneous cable. Confirming our intuition, increasing either the membrane resistance or the intracellular resistivity will increase R_{in}.

Conceptually, we can think of an infinite cable as two semi-infinite cables, one going off to the left and one to the right. The input resistance associated with a single semi-infinite cable R_∞ must therefore be twice the resistance associated with the infinite cable (since current can only flow in one direction); or

$$R_\infty = (r_a \cdot r_m)^{1/2} = r_a\lambda = \frac{r_m}{\lambda} = (R_m R_i)^{1/2}\frac{2}{\pi d^{3/2}}. \tag{2.16}$$

This variable, rather than the resistance associated with an infinite cable, is called R_∞, since it corresponds to the situation of a soma with a single dendrite extending into infinity (Rall, 1959).

The input conductance of a semi-infinite cylinder is given by the inverse of Eq. 2.16,

$$G_\infty = \frac{1}{R_\infty} = \left(\frac{1}{R_m R_i}\right)^{1/2}\frac{\pi d^{3/2}}{2}. \tag{2.17}$$

The input conductance decreases as the square root of the membrane resistance R_m and increases as the $\frac{3}{2}$ power of the diameter of the fiber, a relationship that will be important later on.

The input resistance of a patch of membrane is linearly related to the membrane resistance R_m (with the constant of proportionality given by the total membrane area). In general, as the dimensionality of the space increases, the dependency of the input resistance on R_m lessens. Thus, R_{in} in an infinite cable is proportional to the square root of R_m. For a two-dimensional resistive sheet, $R_{\text{in}} \propto \log(R_m)$. In a three dimensional syncytium (such as muscle tissue) $R_{\text{in}} \propto e^{-1/R_m^{1/2}}$ (see Chap. 3 in Jack, Noble, and Tsien, 1975; Eisenberg and Johnson, 1970). Given the area- or volume-filling geometry of the dendritic tree, the dependency of its input resistance on R_m falls somewhere between that of an infinite cable and that of the resistive sheet.

2.2.2 Finite Cable

Real neurons certainly do not possess infinitely long dendrites, so we need to consider a finite piece of cable of total electrotonic length $L = \ell/\lambda$. The general solution to the

linear second-order ordinary differential cable equation can be expressed in normalized electrotonic units as

$$V(X) = \alpha \cosh(L - X) + \beta \sinh(L - X), \tag{2.18}$$

with $\cosh(x) = (e^x + e^{-x})/2$ and $\sinh(x) = (e^x - e^{-x})/2$. The values of α and β depend on the type of boundary conditions imposed at the two terminals. (What happens at the end of the finite cable influences the voltage throughout the fiber.) We distinguish three different boundary conditions.

Sealed-End Boundary Condition

This is the boundary condition of most relevance to neurons embedded in the living tissue. It assumes that the end of the fiber is covered with neuronal membrane with resistance R_m. It follows that the resistance terminating the equivalent circuit in Fig. 2.3 has the value $4R_m/\pi d^2$. For $d = 2$ μm and $R_m = 10^5$ $\Omega \cdot \text{cm}^2$ this is about 3000 GΩ, a value so high that for all intents and purposes we can consider it to be infinite. If the terminating resistance is infinite, no axial current $I_i(X = L)$ will flow. And since the axial current is given by the derivative of the voltage along the cable, this implies that

$$\left.\frac{dV(X)}{dX}\right|_{X=L} = 0 \tag{2.19}$$

at the terminal. This *zero-slope* or *von Neumann* boundary condition is referred to as a *sealed-end* boundary condition and is the one commonly adopted to model the terminals of dendrites or other neuronal processes. Applying Eq. 2.19 to Eq. 2.18 leads to

$$V(X) = V_0 \frac{\cosh(L - X)}{\cosh(L)}. \tag{2.20}$$

Figure 2.4 illustrates the voltage profile in a short and a long cable with such a sealed-end boundary condition. As expected from Eq. 2.19, the slope of both curves flattens out as the terminal is approached. Furthermore, both curves lie above the voltage decay in a semi-infinite cable. In other words, the voltage in a cable with a sealed end—regardless of its length—decays less rapidly than the voltage in a semi-infinite cable.

We compute the input resistance R_{in} at the origin of the cable, looking into the cable toward its terminal, using the same strategy as in the previous section,

$$R_{\text{in}} = R_\infty \coth(L), \tag{2.21}$$

with $\coth(x) = \cosh(x)/\sinh(x)$. This is plotted in Fig. 2.5 (upper curve). This input resistance is always higher than that of the semi-infinite cable, since the intra-axial current I_i is prevented from leaving the cable at the endpoint of the cable.

Killed-End Boundary Condition

Another type of boundary condition is of relevance when the dendrite or axon is physically cut open or otherwise short-circuited. Under these conditions the intracellular potential at the terminal is identical to the extracellular potential, that is, the effective potential is set to zero,

$$V(X)|_{X=L} = V_L = 0. \tag{2.22}$$

This *Dirichlet* type of boundary condition is also known as *open-* or *killed-end* boundary

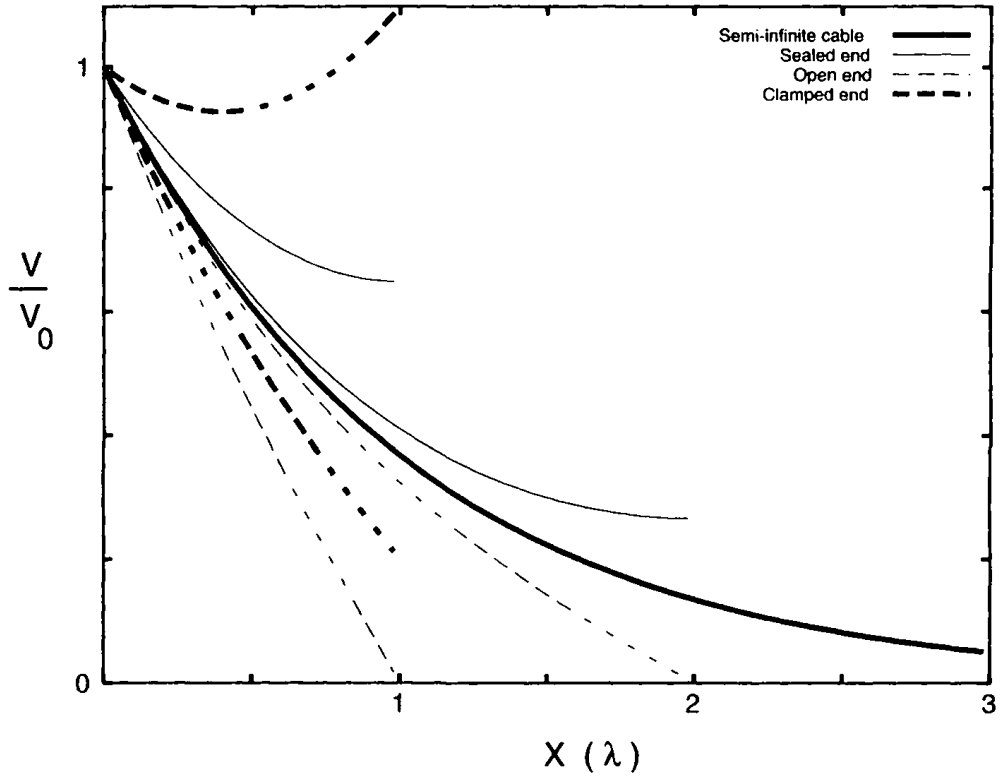

Fig. 2.4 Steady-State Voltage Attenuation Steady-state voltage attenuation in a finite piece of cable as a function of the normalized electrotonic distance $X = x/\lambda$ from the left terminal. The potential at the left terminal is always held fixed at $V = V_0$, while the normalized potential throughout the cable varies with the boundary condition at the right terminal. The bold continuous line corresponds to the voltage in a semi-infinite cable, showing a pure exponential decay. The thin continuous lines show the voltage decay for two cables that terminate in a sealed end (Eq. 2.20) at $X = 1$ or $X = 2$. This is the type of boundary condition used most commonly in simulations. The two thin dashed curves show the same two cables, but now terminating in a short circuit (killed-end boundary condition; Eq. 2.23). Note that either the spatial derivative of voltage (sealed-end) or the voltage itself (killed-end) is zero at the rightmost terminal. That the spatial voltage profile can be nonmonotonic in a passive cable is witnessed by the topmost bold dashed curve, where the voltage at $X = 1$ is clamped to 1.1 times the voltage at the origin. For the lower bold dashed curve, the voltage at the terminal is clamped to $0.2V_0$. Reprinted in modified form by permission from Rall (1989).

condition and corresponds to setting the terminating resistance to zero. It follows that the voltage along the cable is

$$V(X) = \frac{V_0 \sinh(L - X)}{\sinh(L)}, \tag{2.23}$$

and the input resistance is

$$R_{\text{in}} = R_\infty \tanh(L), \tag{2.24}$$

with $\tanh(x) = \sinh(x)/\cosh(x)$. The two thin dashed curves in Fig. 2.4 are the voltage profiles along two cables of electrotonic length $L = 1$ and 2 with a killed-end boundary condition. Their values are always less than the voltage at the corresponding location in a semi-infinite cable. Correspondingly, the input resistance of these cables is always less than that of the semi-infinite cable (Fig. 2.5). The input resistance at the origin $X = 0$ of the

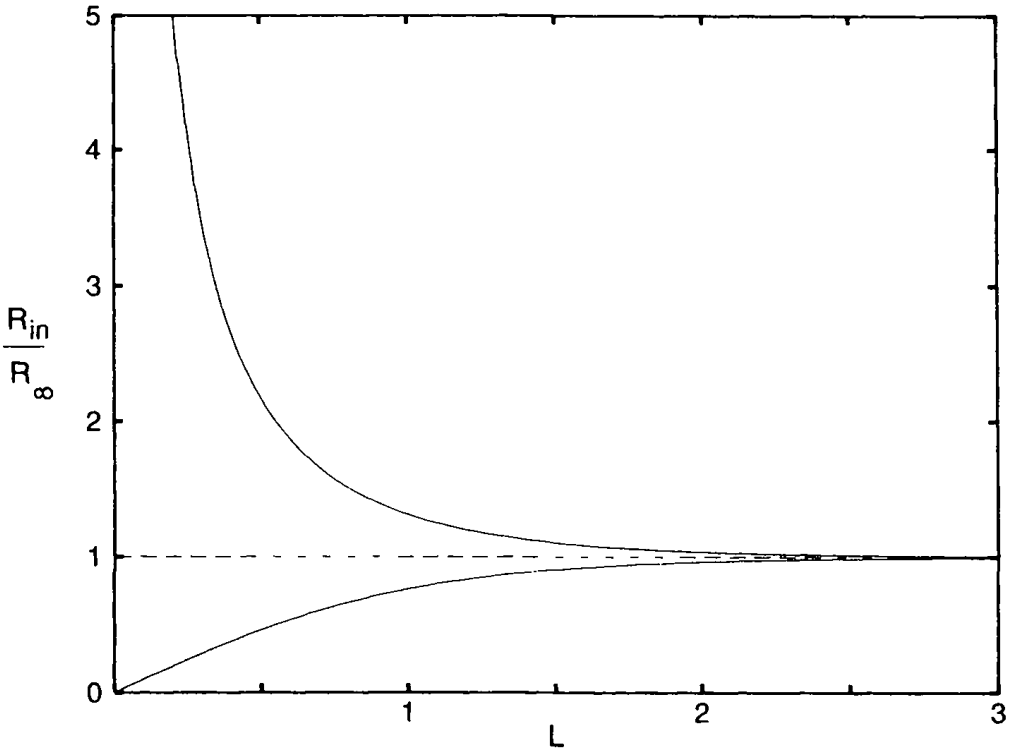

Fig. 2.5 Input Resistance of a Finite Cable Input resistance R_{in} looking into a cable of electrotonic length L toward the right terminal. The ordinate is normalized in terms of the input resistance R_{in} of a semi-infinite cylinder (Eq. 2.16). The normalized input resistance for a sealed-end boundary condition (upper curve) is always larger than R_∞, while the input resistance of a cable with killed-end boundary condition (lower curve) is always less. In the former case, the current is prevented from leaving the cable at the endpoint, while the voltage is "shorted to ground" in the latter case. For cables longer than two space constants, $R_{in} \approx R_\infty$.

cable is inversely proportional (see Eq. 2.2) to the slope of V. The actual input resistance as a function of the electrotonic length of a killed-end cable is shown in Fig. 2.5 (lower curve).

Arbitrary Boundary Condition

In general, the terminal has neither infinite (sealed-end) nor zero (killed-end) resistance, but some finite value R_L. This, for instance, is the case if the cable is connected to some other cable or even to an entire dendritic tree. If we know the value of the voltage at this boundary, that is, V_L, we can express the voltage as

$$V(X) = \frac{V_0 \sinh(L - X) + V_L \sinh(X)}{\sinh(L)}. \tag{2.25}$$

Notice how this expression takes on the value V_0 at $X = 0$ and V_L at $X = L$. In Fig. 2.4 we show two such cases in which V_L is either clamped to $0.2V_0$ or to $1.1V_0$ (causing the non-monotonic appearance). Note that this sagged appearance is a direct consequence of the unusual boundary condition.

The leak current through the terminal follows from Ohm's law and Eq. 2.2 as

$$i_L = \left.\frac{V_L}{R_L}\right|_{X=L} = \left.\frac{-1}{r_a}\frac{dV(X)}{dX}\right|_{X=L}. \tag{2.26}$$

We can now rewrite Eq. 2.25 as

$$V(X) = V_0 \cdot \frac{\cosh(L - X) + (R_\infty / R_L)\sinh(L - X)}{\cosh(L) + (R_\infty / R_L)\sinh(L)}, \tag{2.27}$$

resulting in a general expression for the voltage in a finite piece of cable.

With the help of Eq. 2.3 and the above equation, we can derive an expression for the input resistance of a cable of length L with a terminating resistance R_L,

$$R_{\text{in}} = R_\infty \frac{R_L + R_\infty \tanh(L)}{R_\infty + R_L \tanh(L)}. \tag{2.28}$$

The previous two equations allow us to obtain the values for the voltage and the input resistance for the sealed-end and the killed-end boundary conditions by setting R_L to either ∞ or 0. Furthermore we recover $R_{\text{in}} = R_\infty$ for an infinite cable (since $\tanh(L)$ goes to 1 as $L \to \infty$).

2.3 Time-Dependent Solutions

So far, we have only been concerned with the behavior of the voltage in a cable in response to a stationary current injection, a situation where the voltage settles to a constant value. In general though, we need to consider the voltage trajectory in response to some time-varying current input. Since the time-dependent solution of the cable equation is substantially more complex than the steady-state solution treated above, we will only discuss the solution to two special cases. The interested reader is referred to the monographs by Jack, Noble, and Tsien (1975) and by Tuckwell (1988a) for a treatment of many more cases of interest.

Before we do so, we will introduce a normalized version of the cable equation. Recalling the definition of the neuronal time constant from Chap. 1 as

$$\tau_m = r_m c_m = R_m C_m \tag{2.29}$$

allows us to introduce dimensionless variables for both time, $T = t/\tau_m$, and space, $X = x/\lambda$. Written in these units and taking care to properly transfrom the input current (Sec. 4.4 in Tuckwell, 1988a), the cable equation becomes

$$\frac{\partial^2 V(X,T)}{\partial X^2} = \frac{\partial V(X,T)}{\partial T} + V(X,T) - \frac{I_{\text{inj}}(X,T)}{\lambda c_m}, \tag{2.30}$$

with $I_{\text{inj}}(X,T) = \lambda \tau_m I_{\text{inj}}(x,t)$ and $I_{\text{inj}}(x,t)$ corresponds to the stimulus current density.

2.3.1 Infinite Cable

In order to compute the dynamic behavior of the infinite cable in response to current injections we will once again exploit the linearity of Eq. 2.30, that is, the fact that if the response of the membrane to the current $I(X,T)$ is $V(X,T)$, the polarization in response to the current $\alpha I(X,T)$ is $\alpha V(X,T)$.

Voltage Response to a Current Pulse

As discussed in the first chapter (and summarized in Appendix B), we can completely characterize the system by computing the *impulse response* or *Green's function* associated with Eq. 2.30, which we do by transforming to the Fourier domain, assuming that $V(X) \to 0$ as $|X| \to \infty$, and transferring back to the time domain (Jack, Noble, and Tsien, 1975).